REFERENCES

Aneli, J.N., Zaikov, G.E., and Khananashvili, L.M. (1999) Effects of mechanical deformations on the structurization and electric conductivity of electric conducting polymer composites. Journal of Applied Polymer Science, 74, 601-621.

Bunsomsit, K., Magaraphan, R., O'Rear, E.A., and Grady, B.P. (2002) Polypyrrole-coated natural rubber latex by admicellar polymerization. Colloid Polym Sci, 280, 509–516.

Genetti, W.B., Yuan, W.L., Grady, B.P., and O'Rear, E.A. (1998) Polymer matrix composites: Conductivity enhancement through polypyrrole coating of nickel flake, J Mater Sci, 33, 3085-3093.

Job, A.E., Oliveira, F.A., Alves, N., Giacometti, J.A., and Mattoso, L.H.C. (2003) Conductive composites of natural rubber and carbon black for pressure sensors. Synthetic Metals, 135-136, 99-100.

Kudoh, Y. (1996) Properties of polypyrrole prepared by chemical polymerization using aqueous solution containing $Fe_2(S0_4)_3$ and anionic surfactant. Synthetic Metals, 79, 17-22.

Lee, J.Y., Kim, D.Y., and Kim, C.Y. (1995) Synthesis of soluble polypyrrole of the doped state in organic solvents. Synthetic Metals, 74, 103-106.

Lee, J.Y., Song, K.T., Kim, S.Y., Kim, D.Y., and Kim. C.Y. (1997) Synthesis and characterization of soluble polypyrrole. Synthetic Metals, 84, 137-140.

Liu, J., and Wan. M. (2001) Polypyrrole doped with 1,5-naphthalenedisulfonic acid. Synthetic Metals, 124, 317-321.

Mano, V., Felisberti, M.I., Matencio, T., and Paolit, M.D. (1996) Thermal, mechanical and electrochemical behaviour of poly(vinyl chloride) /polypyrrole blends (PVC/PPy). Polymer, 37(23), 5165-5170.

Nakason, C., Kaesaman, A., and Eardrod, K. (2005) Cure and mechanical properties of natural rubber-g-poly(methyl methacrylate)–cassava starch compounds. Materials Letters, 59, 4020 – 4025.

Nontasorn, P., Chavadej, S., Rangsunvigit, P., O'Haver, J.H., Chaisirimahamorakot, S., and Na-Ranong, N. (2005) Admicellar polymerization modified silica

via a continuous stirred-tank reactor system: Comparative properties of rubber compounding. Chemical Engineering Journal, 108, 213–218.

Okuzaki, H., Hattori, T., Morikage, H., and Yamada, Y. (2005) Electrically induced contraction of zone-drawn polypyrrole films. Synthetic Metals, 153, 105-108.

Omastova, M., Trchova, M., Kovarova, J., and Stejskal, J. (2003) Synthesis and structural study of polypyrroles prepared in the presence of surfactants. Synthetic Metals, 138, 447–455.

Pongprayoon, T., Yanumet, N., and O'Rear, E.A. (2002) Admicellar Polymerization of Styrene on Cotton. Journal of Colloid and Interface Science, 249, 227–234.

Rippel, M.M., Lee,L., Leite, C.A.P., and Galembeck F. (2003) Skim and cream natural rubber particles: colloidal properties, coalescence and film formation. Journal of Colliod and Interface Science, 268, 330-340.

Rosen, M.J. (2004) Surfactants and Interfacial Phenomena. New Jersy: John Wiley & Sons, Inc.

Roy, R.V., Das, M., Banerjee, R., and Bhowmick, A.K. (2006) Comparative studies on crosslinked and uncrosslinked natural rubber biodegradation by *Pseudomonas* sp.. Bioresource Technology, 97, 2485-2488.

Rungruang, P., Grady, B.P., and Supaphol, P. (2006) Surface-modified calcium carbonate particles by admicellar polymerization to be used as filler for isotactic polypropylene. Colloids and Surfaces A: Physicochem. Eng. Aspects, 275, 114–125.

Sahin, D., Sari, B., and Unal, H.I. (2002) An investigation of some parameters on electrorheologocal properties of polyprrole suspensions. Turk J Chem, 26, 113-124.

Sau, K.P., Chaki, T.K., and Khastgir, D. (1998) The change in conductivity of a rubber-carbon black composite subjected to different modes of pre-strain. Composites Part A, 29A, 363-370.

Shen, Y., and Wan, M. (1998) In situ doping polymerization of pyrrole with sulfonic acid as a dopant. Synthetic Metals, 96, 127-132.

Song, K.T., Lee, J.Y., Kim, H.D., Kim, D.Y., Kim, S.Y., and Kim, C.Y. (2000) Solvent effects on the characteristics of soluble polypyrrole. Synthetic Metals, 110, 57-63.

Song, M.K., Kim, Y.T., Kimb, B.S., Kim, C., Char, K., and Rhee, H.W. (2004) Synthesis and characterization of soluble polypyrrole doped with alkylbenzenesulfonic acids. Synthetic Metals, 141, 315–319.

surfactant bilayers in the formation of ultrathin films . Langmuir, 3, 531-537.

Vilcakova, J., Paligova, M., Omastova, M., Saha, P. and Quadrat, O. (2004) Switching effect in pressure deformation of silicone rubber/polypyrrole composites. Synthetic Metals, 146, 121-126.

Vilcakova, J., Paligova, M., Omastova, M., Saha, P., and Quadrat, O. (2004) Switching effect in pressure deformation of silicone rubber/polypyrrole composites. Synthetic Metals, 146,121-126.

Vishnuvardhan, T.K., Kulkarni, V.R., Basavaraja, C., and Raghavandra, S.C. (2006) Synthesis, characterization and a.c. conductivity of polypyrrole/Y_2O_3 composites. Bull. Mater. Sci., 29, 77-83.

Wang, L.X., Li, X.G., and Yang, Y.L. (2001) Preparation, properties and applications of polypyrroles. Reactive & Functional Polymers, 47, 125–139.

Wu, J., Harwell, J.H., and O'Rear, E.A. (1987) Two-dimensional reaction solvents: surfactant bilayers in the formation of ultrathin films. Langmuir, 3, 531-537.

Wu, J., Zhou, D., Tou, C.O., and Wallace, G.G. (2005) Conducting polymer coated lycra. Synthetic Metals, 155, 698-701.

Xie, H.-Q., and Ma, Y.M. (2000) Change of conductivity of polyaniline/(styrene-butadiene-styrene) triblock copolymer composites during mechanical deformation. Journal of Applied Polymer Science, 77, 2156-2164.

Yan, F., Xue, G. and Wan X. (1999) Liquid polysulfide rubber as a new dopant of polypyrrolr. Synthetic Metals, 107, 35-38.

APPENDICES

Appendix A Admicelled Latex Recipe

Table A1 Ingredients of the admicelled rubbers

Sample	SDS (mM)	SDS (g)	NaCl (M)	NaCl (g)	Pyrrole (mM)	Pyrrole (μL)	$Fe_2(SO_4)_3$ (mM)	$Fe_2(SO_4)_3$ (g)
A2,1-1	16	2.307	0	0.0	20	691.6	20.0	3.9988
A2,2-1	16	2.307	0	0.0	20	691.6	10.0	1.9994
A2,3-1	16	2.307	0	0.0	20	691.6	6.7	1.3329
A5,1-1	16	2.307	0	0.0	50	1729.1	50.0	9.9970
A5,2-1	16	2.307	0	0.0	50	1729.1	25	4.9985
A5,3-1	16	2.307	0	0.0	50	1729.1	16.7	3.3323
A10,1-1	16	2.307	0	0.0	100	3458.2	100.0	19.9940
A10,2-1	16	2.307	0	0.0	100	3458.2	50.0	9.9970
A10,3-1	16	2.307	0	0.0	100	3458.2	33.3	6.6647
B2,1-1	5.6	0.8074	0.1	2.9222	20	691.6	20.0	3.9988
B2,2-1	5.6	0.8074	0.1	2.9222	20	691.6	10.0	1.9994
B2,3-1	5.6	0.8074	0.1	2.9222	20	691.6	6.7	1.3329
B5,1-1	5.6	0.8074	0.1	2.9222	50	1729.1	50.0	9.9970
B5,2-1	5.6	0.8074	0.1	2.9222	50	1729.1	25	4.9985
B5,3-1	5.6	0.8074	0.1	2.9222	50	1729.1	16.7	3.3323
B10,1-1	5.6	0.8074	0.1	2.9222	100	3458.2	100.0	19.9940
B10,2-1	5.6	0.8074	0.1	2.9222	100	3458.2	50.0	9.9970
B10,3-1	5.6	0.8074	0.1	2.9222	100	3458.2	33.3	6.6647
C2,1-1	3.2	0.4614	0.3	8.7665	20	691.6	20.0	3.9988
C2,2-1	3.2	0.4614	0.3	8.7665	20	691.6	10.0	1.9994
C2,3-1	3.2	0.4614	0.3	8.7665	20	691.6	6.7	1.3329
C5,1-1	3.2	0.4614	0.3	8.7665	50	1729.1	50.0	9.9970
C5,2-1	3.2	0.4614	0.3	8.7665	50	1729.1	25	4.9985
C5,3-1	3.2	0.4614	0.3	8.7665	50	1729.1	16.7	3.3323
C10,1-1	3.2	0.4614	0.3	8.7665	100	3458.2	100.0	19.9940
C10,2-1	3.2	0.4614	0.3	8.7665	100	3458.2	50.0	9.9970
C10,3-1	3.2	0.4614	0.3	8.7665	100	3458.2	33.3	6.6647

Note Total volume of the reaction is 500 ml.

Ax,y-z:

A,B,C = [NaCl] 0.0, 0.1, 0.3 M, x = [PPy] 20, 50, 100 mM, y-z = [Mo]/[In]

Table A2 Calculation of pyrrole content in the admicelled rubbers in gram

Pyrrole (mM)	**Pyrrole** (g)	**Latex** (g)	**Pyrrole** (wt%)	**Latex** (wt%)
20	0.5706	25	2.61	97.39
50	1.6773	25	6.29	93.71
100	3.3545	25	11.83	88.17

Note

Total volume of the reaction is 500 ml.

Appendix B Calculation for Volume and Surface Resistivity

Surface Resistivy

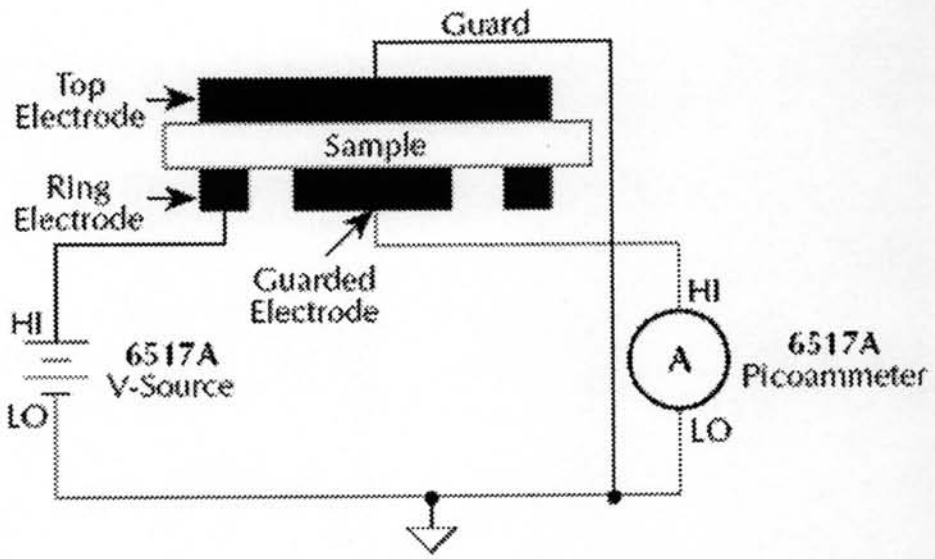

Figure B1 Surface resistivity measurement technique.

$$\rho_s = K_s R$$

ρ_s = surface resistivity (per square)

R = measured resistance in ohms (V/I)

$K_s = P/g$

where:

P = the effective perimeter of the guarded electrode (mm)

g = distance between the guarded electrode and the ring electrode(mm).

For circular electrodes:

$P = \pi D_0$

$D_0 = D_1 + g$

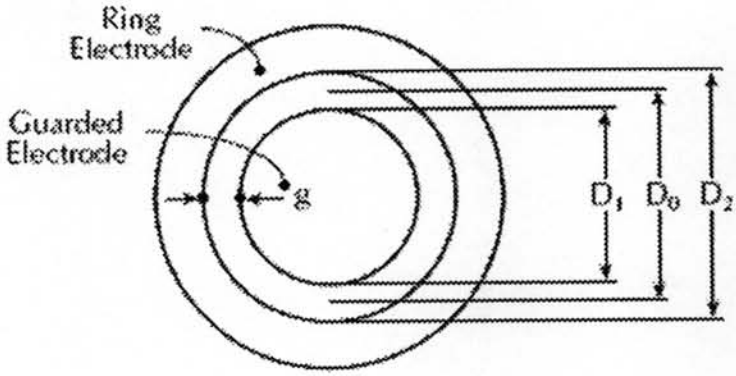

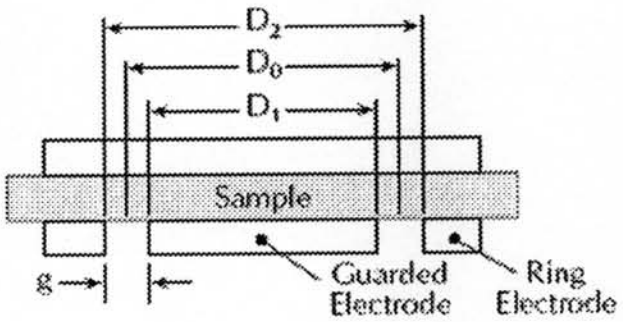

Test Fixture Dimensions (cm)	
	Model 8009
D_1	2.000 in
D_0	2.125 in
D_2	2.250 in
g	0.125 in

Figure B2 Circular electrode dimensions.

Volume Resistivity

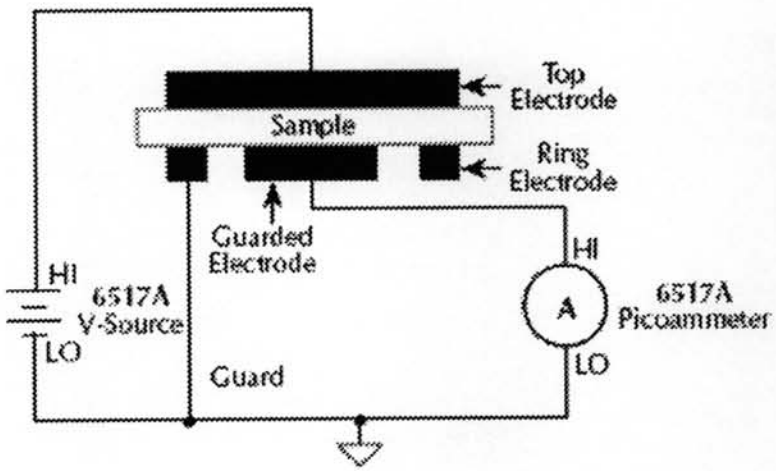

Figure B3 Volume resistivity measurement technique.

$$\rho_v = \frac{K_v}{\tau} R$$

ρ_v = surface resistivity (per square)

K_v = the effective area of the guarded electrode for the particular electrode arrangement employed

τ = average thickness of the sample (mm)

R = measured resistance in ohms (V/I)

For circular electrodes:

$$K_v = \pi(\frac{D_1}{2} + B\frac{g}{2})^2$$

D_1 = outside diameter of guarded electrode

g = distance between the guarded electrode and the ring electrode

B = effective area coefficient, B of 0 is typically used for volume resistivity

Appendix C Data of Particle Size Distribution

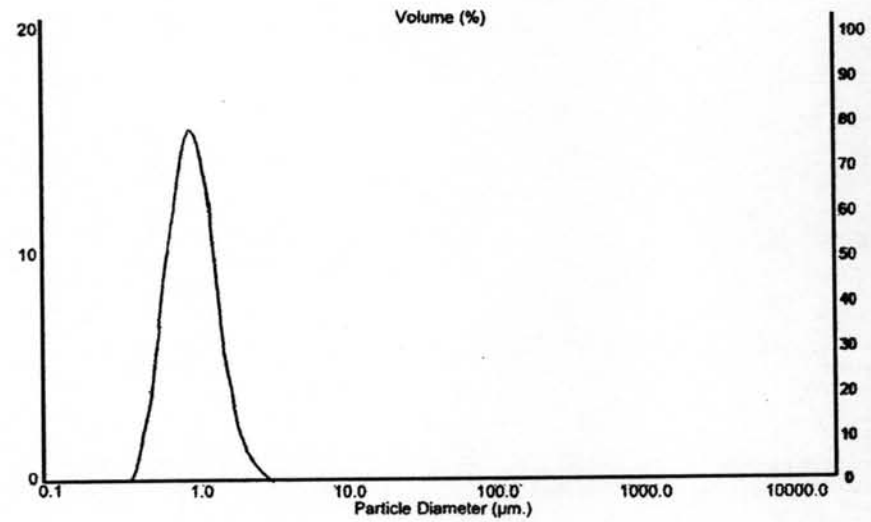

Figure C1 Histogram showing the particle size distribution by volume of the natural rubber latex.

Appendix D Data of Electrophoretic Mobility

Table D1 Mean electrophoretic mobility of centrifuged NR latex

pH	EM (microns/sec per volt/cm)
3.0	3.242
3.6	1.802
4.0	-1.554
4.5	-3.318
6.2	-4.068

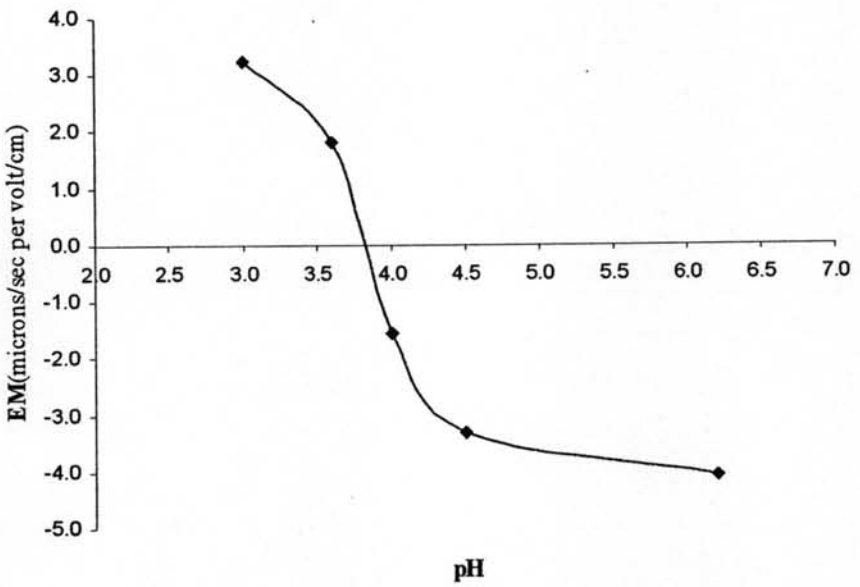

Figure D1 The electrophoretic mobility of charged latex particles in aqueous solution at various pH.

Appendix E Scanning Electron Micrographs of the Admicelled Rubbers

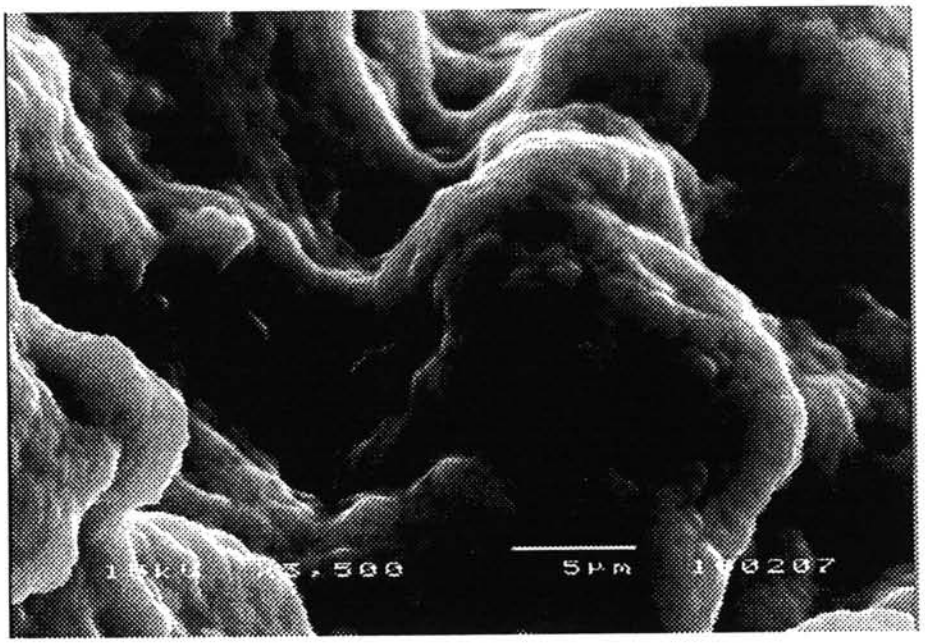

Figure E1 Scanning electron micrograph of B20,1-1 at magnification 3500/15 kV.

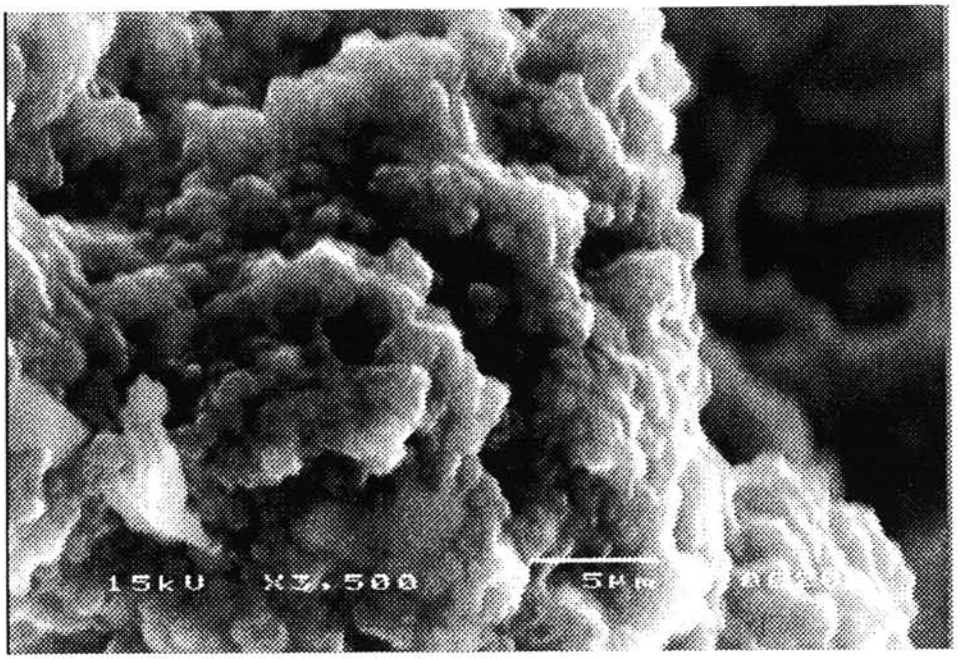

Figure E2 Scanning electron micrograph of B50,1-1 at magnification 3500/15 kV.

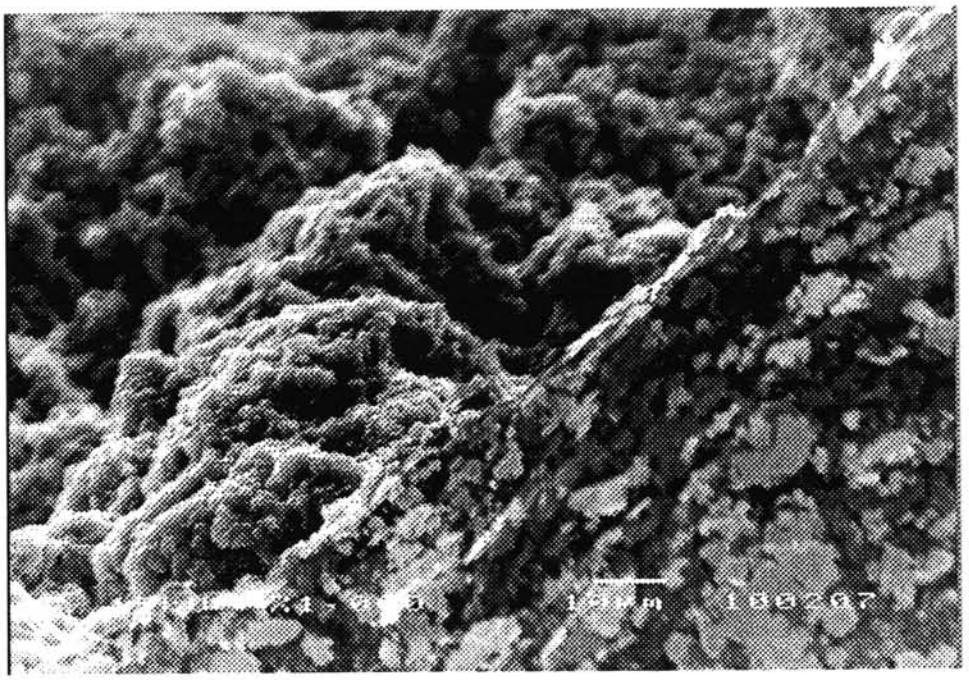

Figure E3 Scanning electron micrograph of B100,1-1 at magnification 1000/15 kV.

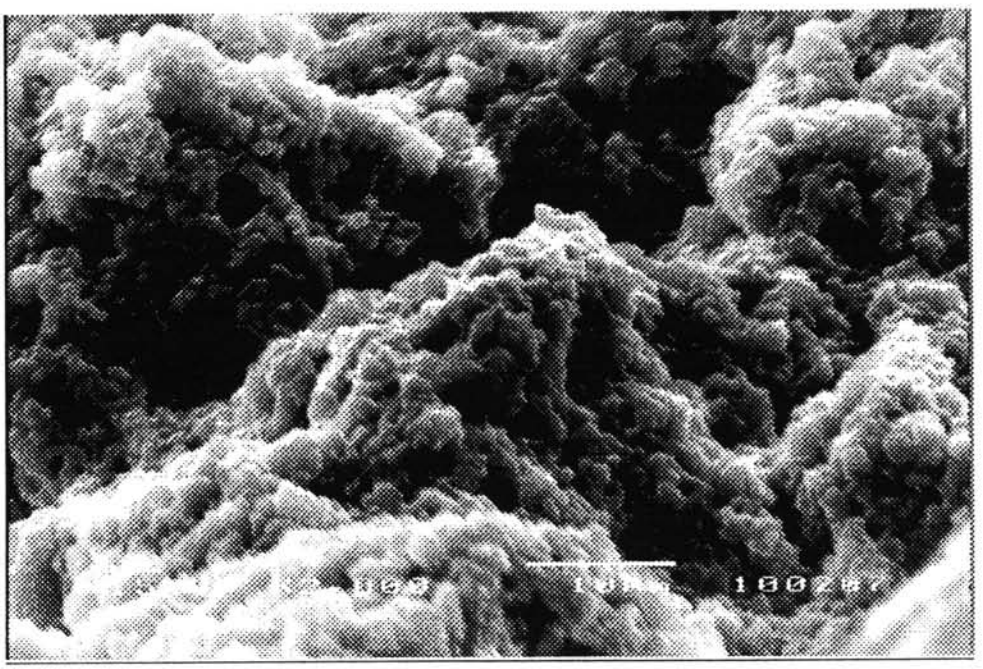

Figure E4 Scanning electron micrograph of B100,1-1 at magnification 2000/15 kV.

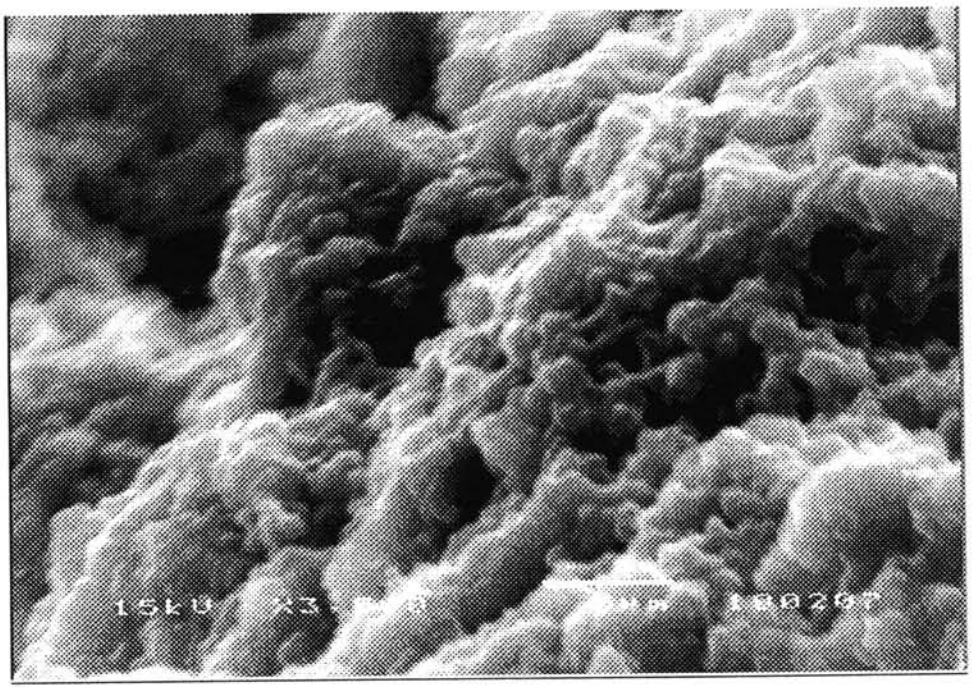

Figure E5 Scanning electron micrograph of B100,1-1 at magnification 3000/15 kV.

Appendix F Data of Thermogravimetric Analysis

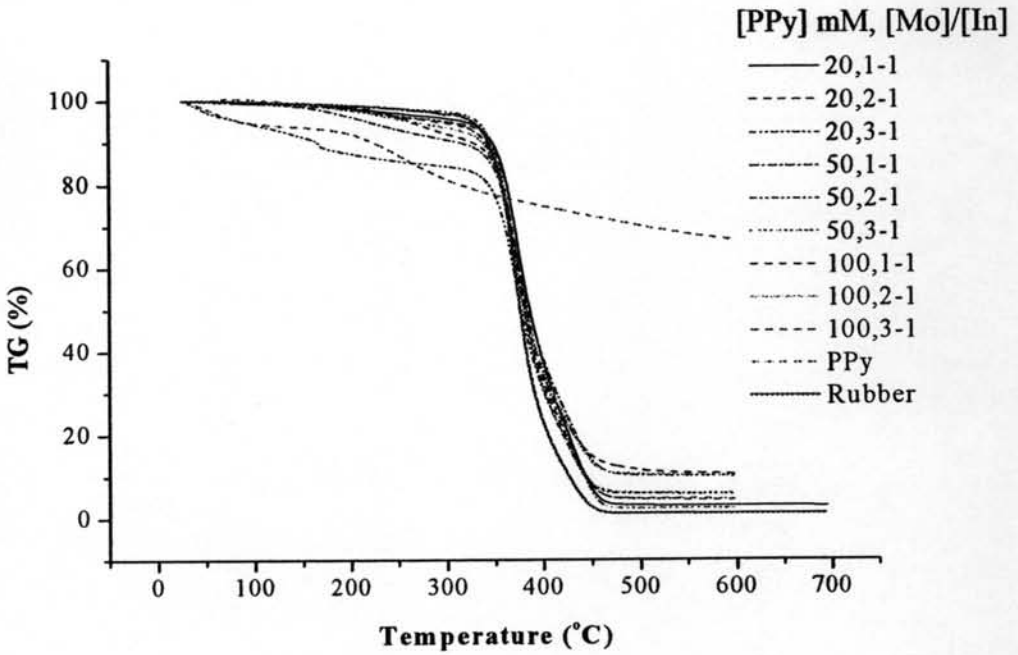

Figure F1 Thermogravimetric analysis thermograms at 10 °C/min of nitrogen atmosphere of the admicelled rubbers without salt.

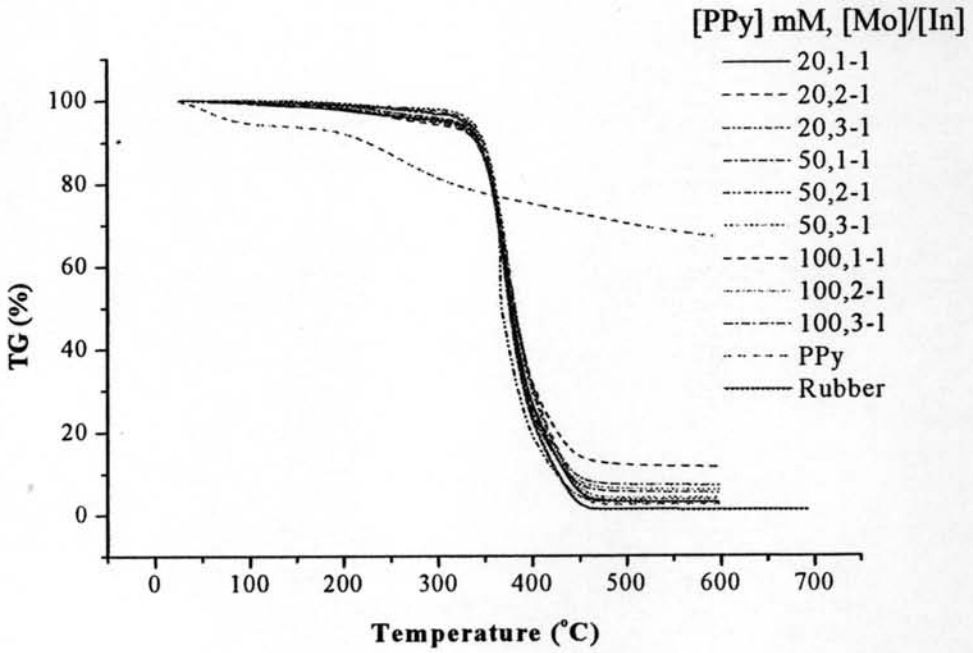

Figure F2 Thermogravimetric analysis thermograms at 10 °C/min of nitrogen atmosphere of the admicelled rubbers with 0.1M NaCl.

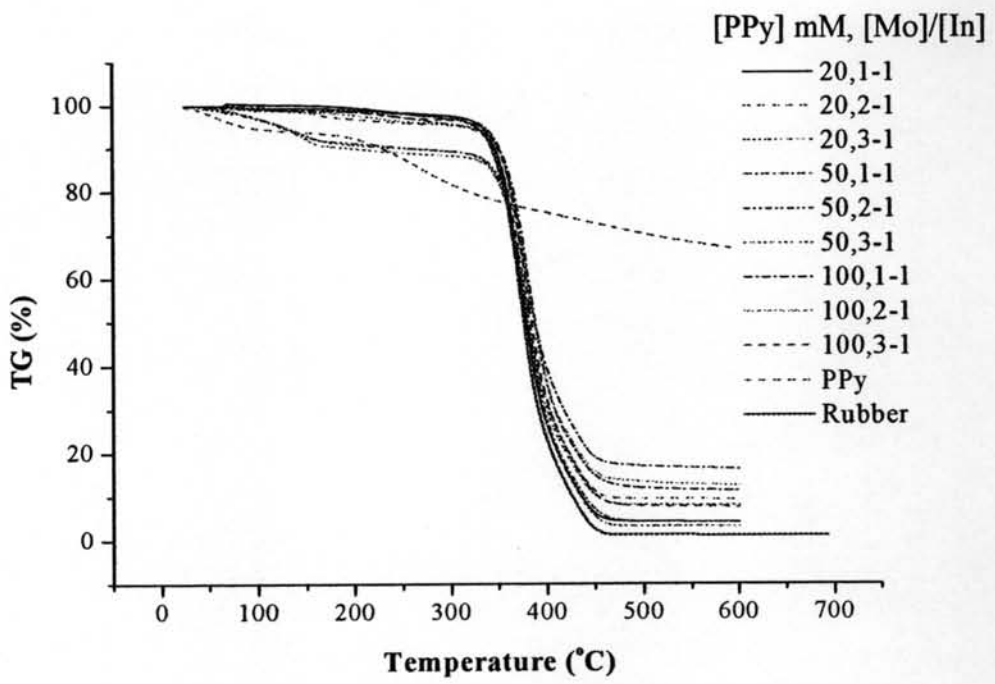

Figure F3 Thermogravimetric analysis thermograms at 10 °C/min of nitrogen atmosphere of the admicelled rubbers with 0.3M NaCl.

Appendix G Data of Fourier-Transform Infrared Spectroscopy

Table G1 FT-IR peak assignments for the IR absorption band

Wavenumber (cm^{-1})	Assignment
Rubber	
3035	=C-H stretching
2960	C-H stretching of CH_3
2926	C-H stretching of CH_2
2853	C-H stretching of CH_2 and CH_3
1663	C=C stretching
1448	C-H bending of CH_2
1375	C-H bending of CH_3
1128	C-H bending
834	C=CH wagging
Polypyrrole	
1557	C=C stretching
1476	C-C stretching
1285,1193	=C-H in plane
1044	N-H in plane
924	C-H stretching
787	=C-H out of plane
684	C-C out of plane
618	N-H out of plane

Appendix H Data of Mechanical Properties Measurement

Table H1 Raw data of tensile properties

Sample	Thickness (mm)	Elongation at break (%)	Tensile strength (MPa)	Young's modulus (MPa)
A20,1-1	0.8892	107±22	0.94±0.21	0.89±0.95
A20,2-1	0.3258	149±43	1.08±0.04	0.73±0.09
A20,3-1	0.7243	171±37	0.45±0.09	0.26±0.24
A50,1-1	0.2646	72±9	1.99±0.13	2.88±1.18
A50,2-1	0.276	208±50	2.73±0.12	1.35±0.24
A50,3-1	0.6657	163±12	0.81±0.08	0.50±0.66
A100,1-1	0.4363	39±4	3.98±0.28	11.03±6.37
A100,2-1	0.598	48±10	0.56±0.08	1.40±0.57
A100,3-1	0.592	88±13	1.47±0.07	1.70±0.45
B20,1-1	0.5618	113±15	1.63±0.13	1.44±0.88
B20,2-1	0.675	199±21	0.64±0.10	0.39±0.12
B20,3-1	0.7047	120±29	1.44±0.33	1.20±1.11
B50,1-1	0.4258	118±4	2.62±0.32	2.28±5.02
B50,2-1	0.4091	102±11	1.42±0.16	1.40±1.35
B50,3-1	0.651	88±14	1.41±0.30	1.62±2.15
B100,1-1	0.3593	51±8	8.40±0.45	16.79±5.48
B100,2-1	0.3058	83±15	4.24±0.20	5.16±1.32
B100,3-1	0.5008	69±5	2.29±0.22	3.37±3.65
C20,1-1	0.8967	133±5	0.58±0.01	0.44±0.16
C20,2-1	0.9242	69±14	0.43±0.08	0.62±0.57
C20,3-1	0.6192	73±10	0.55±0.04	0.76±0.41
C50,1-1	0.4293	139±15	2.68±0.34	1.95±2.20
C50,2-1	0.5425	54±10	1.99±0.32	3.72±3.14
C50,3-1	0.5208	78±16	1.59±0.16	2.05±0.99

Sample	Thickness (mm)	Elongation at break (%)	Tensile strength (MPa)	Young's modulus (MPa)
C100,1-1	0.3375	48±15	4.12±0.58	9.87±3.03
C100,2-1	0.4936	127±21	2.70±0.55	2.17±2.35
C100,3-1	0.7655	88±21	1.81±0.41	2.07±1.96
Rubber	1.2	447±8	0.23±0.06	0.01±0.47

Note

Ax,y-z:

A,B,C = [NaCl] 0.0, 0.1, 0.3 M, x = [PPy] 20, 50, 100 mM, y-z = [Mo]/[In]

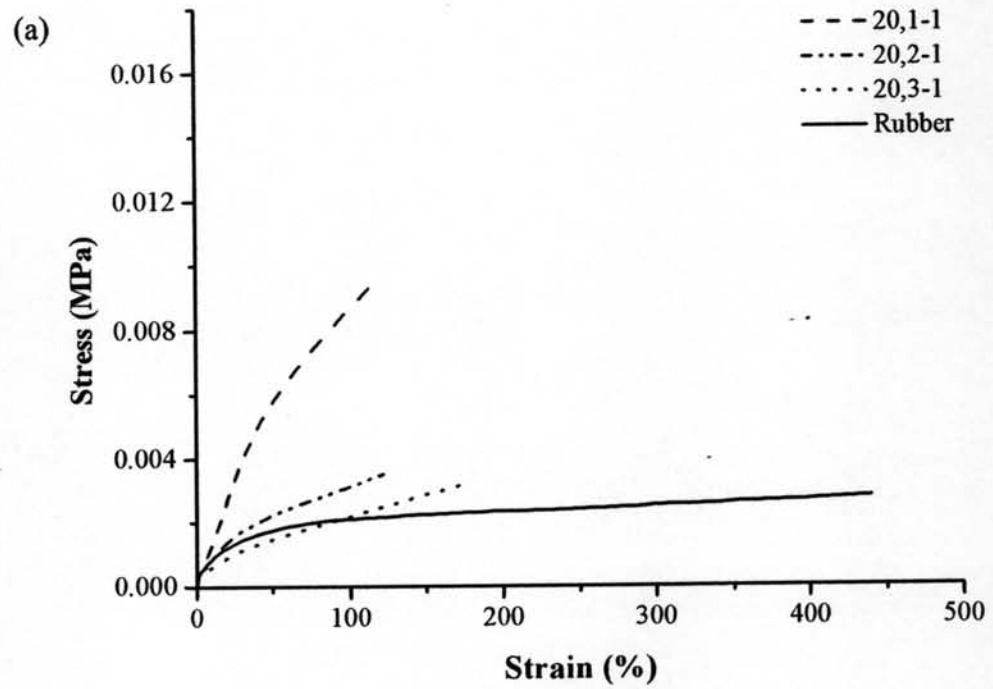

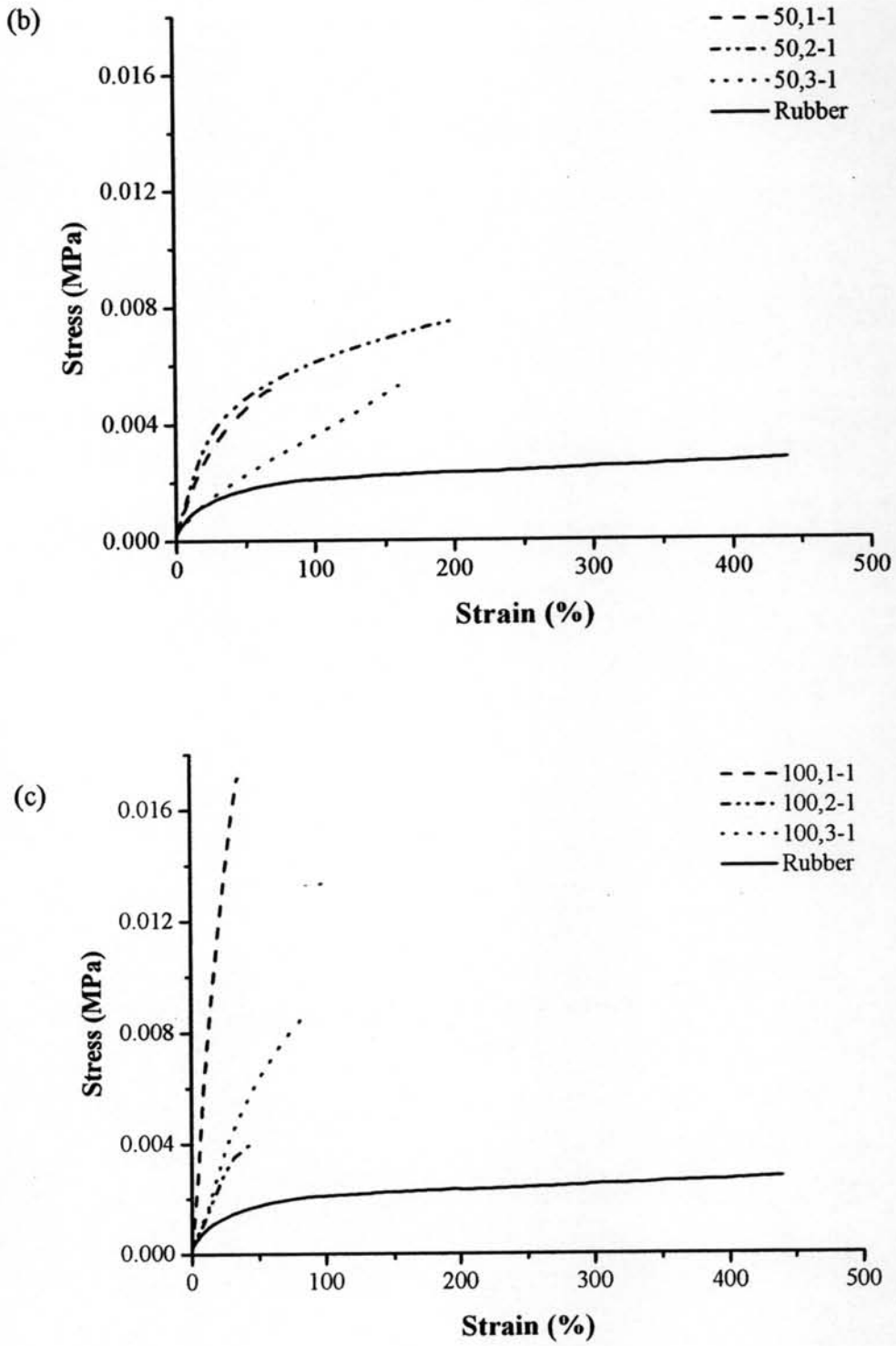

Figure H1 Effect of [Mo]:[In] on the Stress-Strain curves of the admicelled rubbers with no salt (a) PPy 20 mM, (b) PPy 50 mM, (c) PPy 100 mM.

(a)

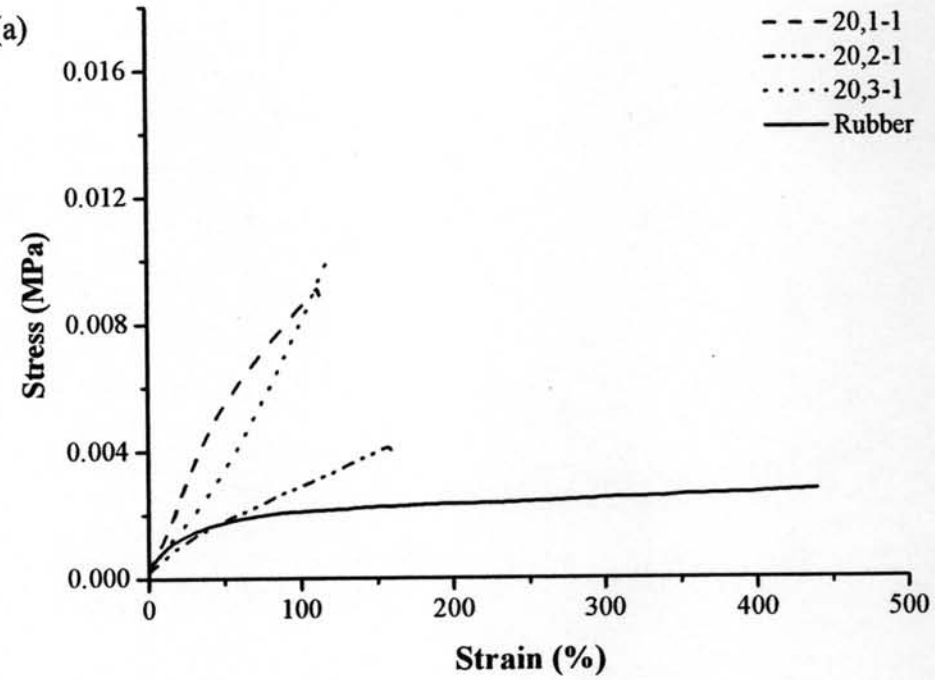
20,1-1
20,2-1
20,3-1
Rubber
Stress (MPa)
0.016
0.012
0.008
0.004
0.000
0
100
200
300
400
500
Strain (%)

(b)

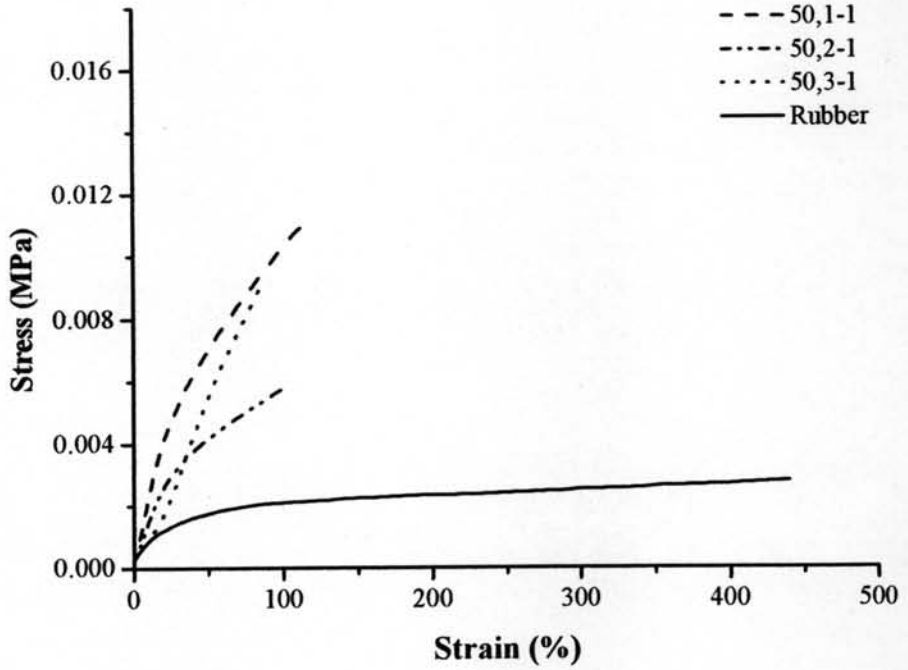
50,1-1
50,2-1
50,3-1
Rubber
Stress (MPa)
0.016
0.012
0.008
0.004
0.000
0
100
200
300
400
500
Strain (%)

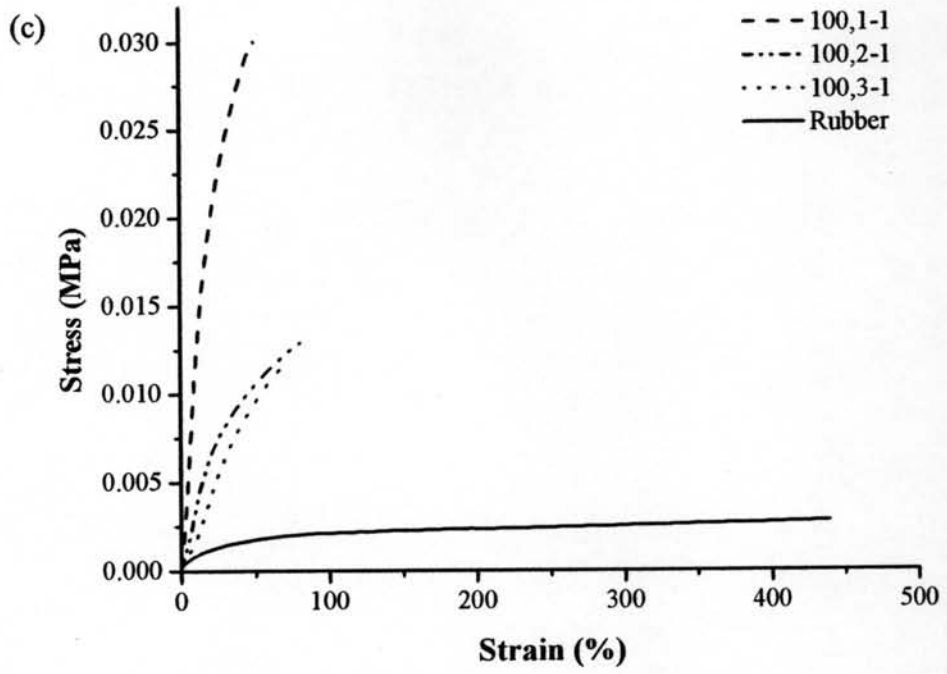

Figure H2 Effect of [Mo]:[In] on the Stress-Strain curves of the admicelled rubbers with 0.1M NaCl (a) PPy 20 mM, (b) PPy 50 mM, (c) PPy 100 mM.

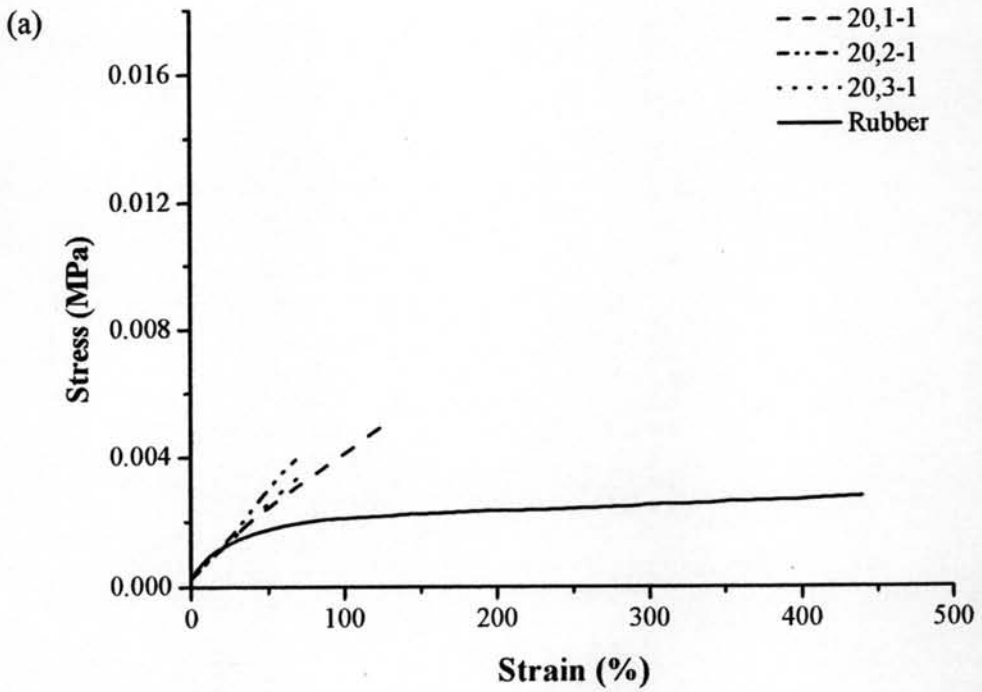

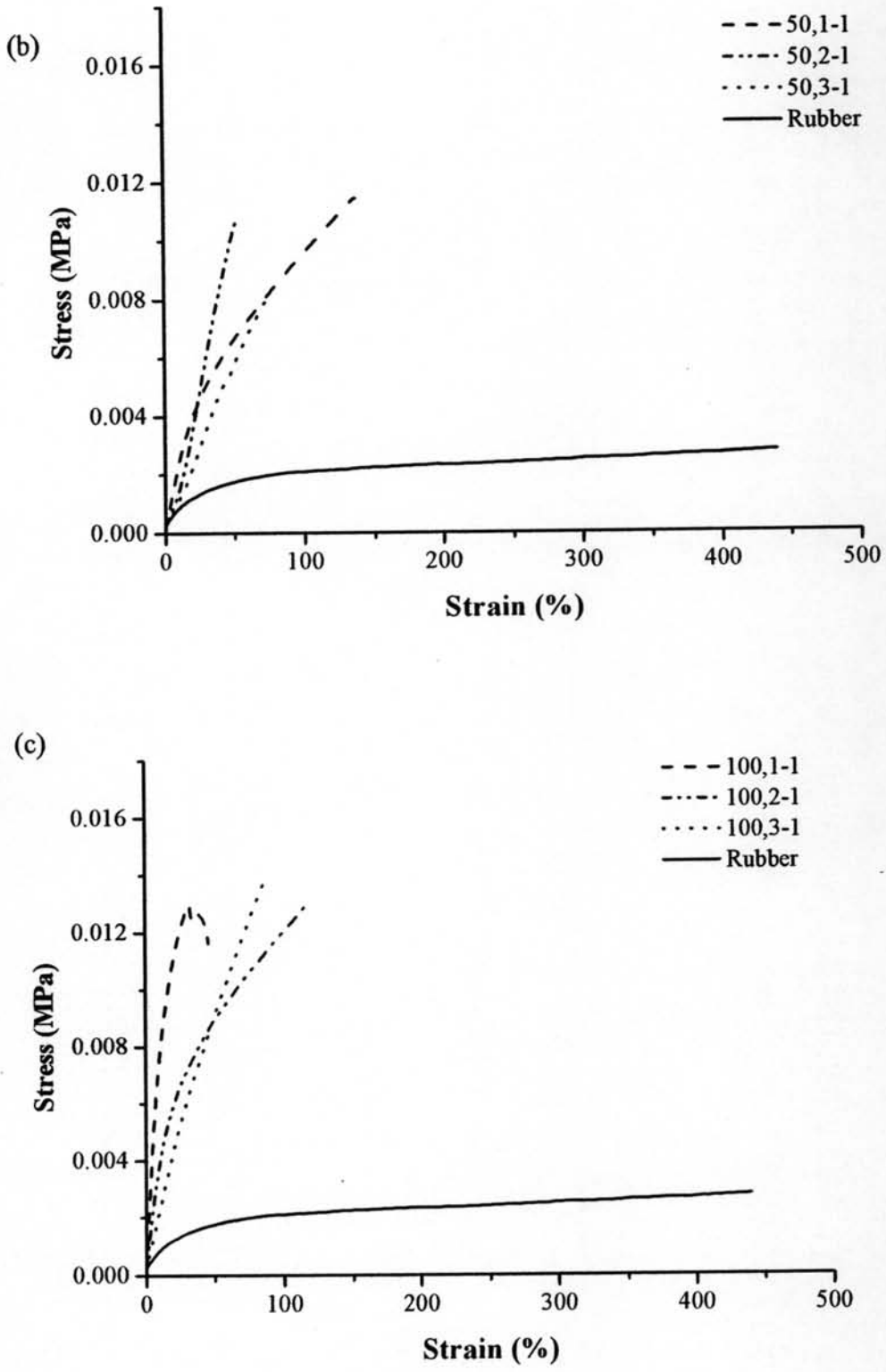

Figure H3 Effect of [Mo]:[In] on the Stress-Strain curves of the admicelled rubbers with 0.3M NaCl (a) PPy 20 mM, (b) PPy 50 mM, (c) PPy 100 mM.

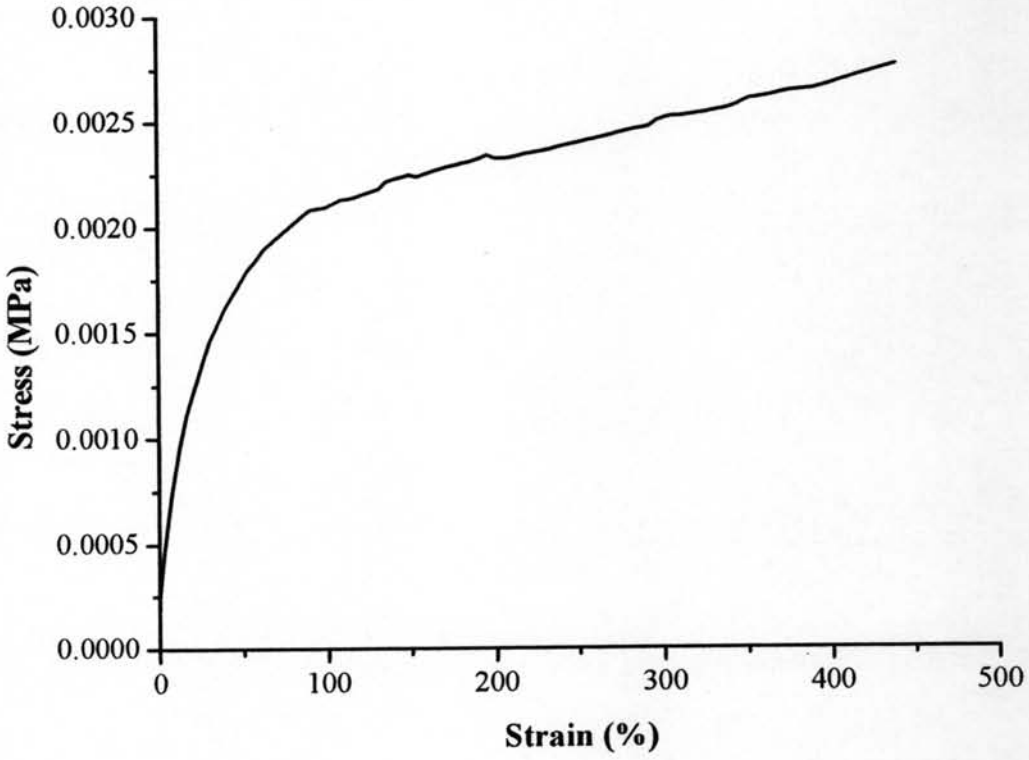

Figure H4 Stress-Strain curve of natural rubber.

Appendix I Data of Dynamic Mechanical Analysis

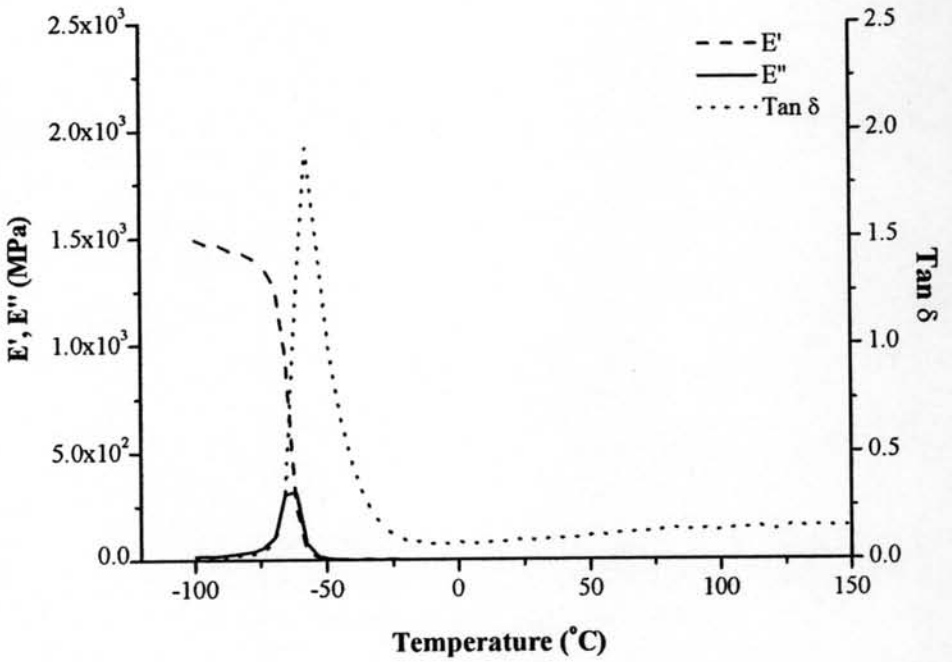

Figure I1 Storage modulus, loss modulus and tan δ of A20,1-1.

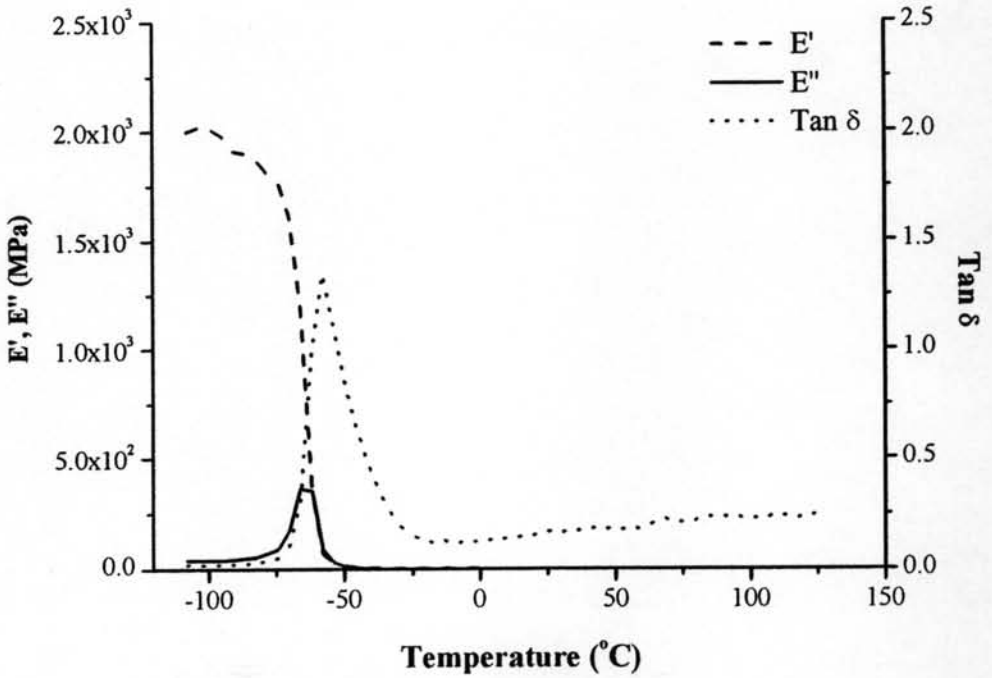

Figure I2 Storage modulus, loss modulus and tan δ of A20,2-1.

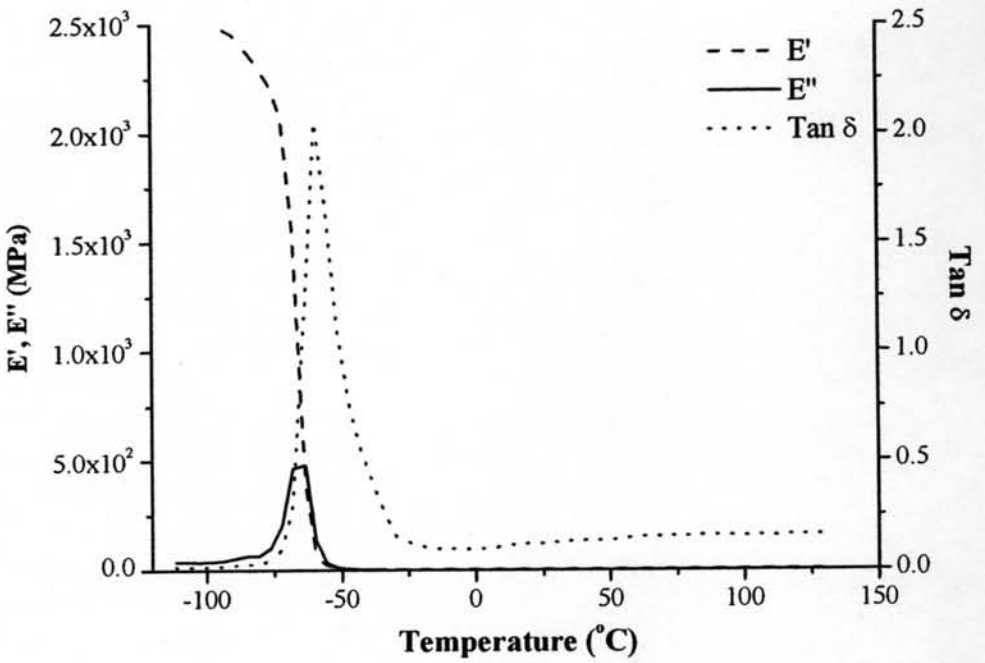

Figure I3 Storage modulus, loss modulus and tan δ of A20,3-1.

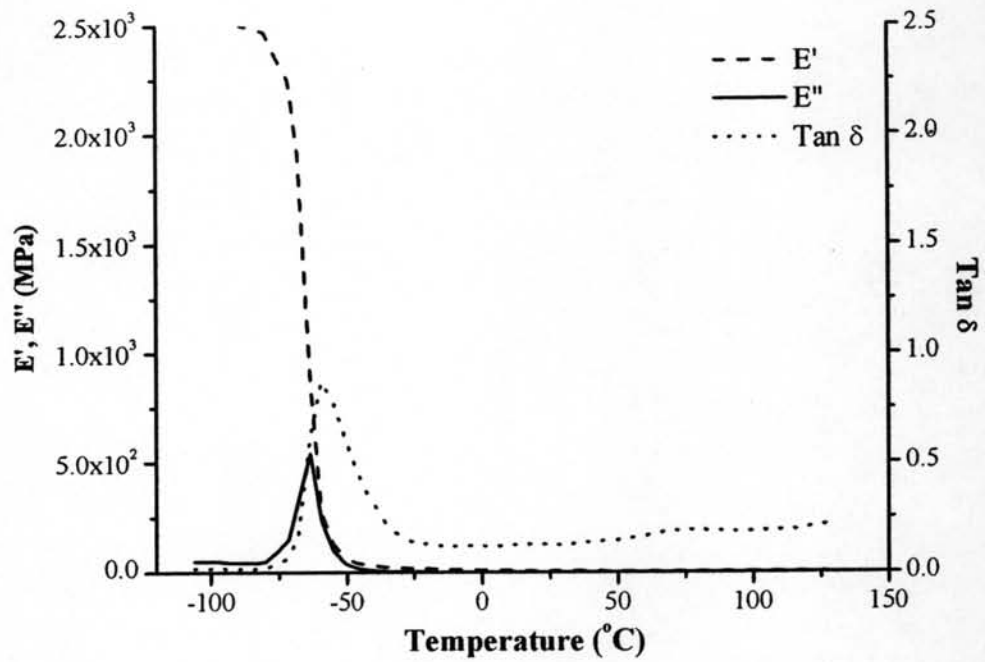

Figure I4 Storage modulus, loss modulus and tan δ of A50,1-1.

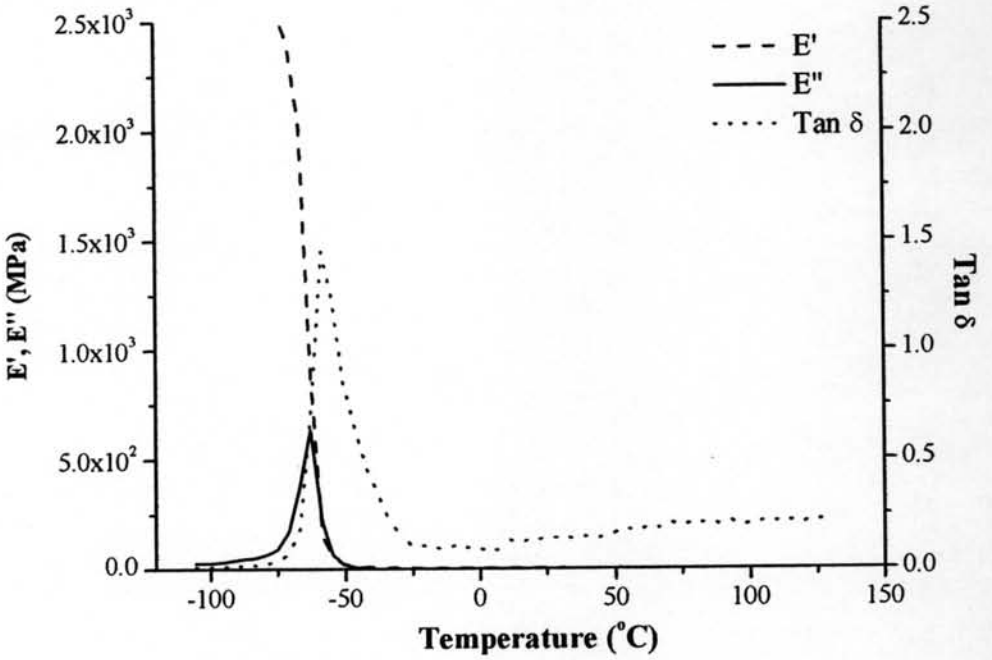

Figure I5 Storage modulus, loss modulus and tan δ of A50,2-1.

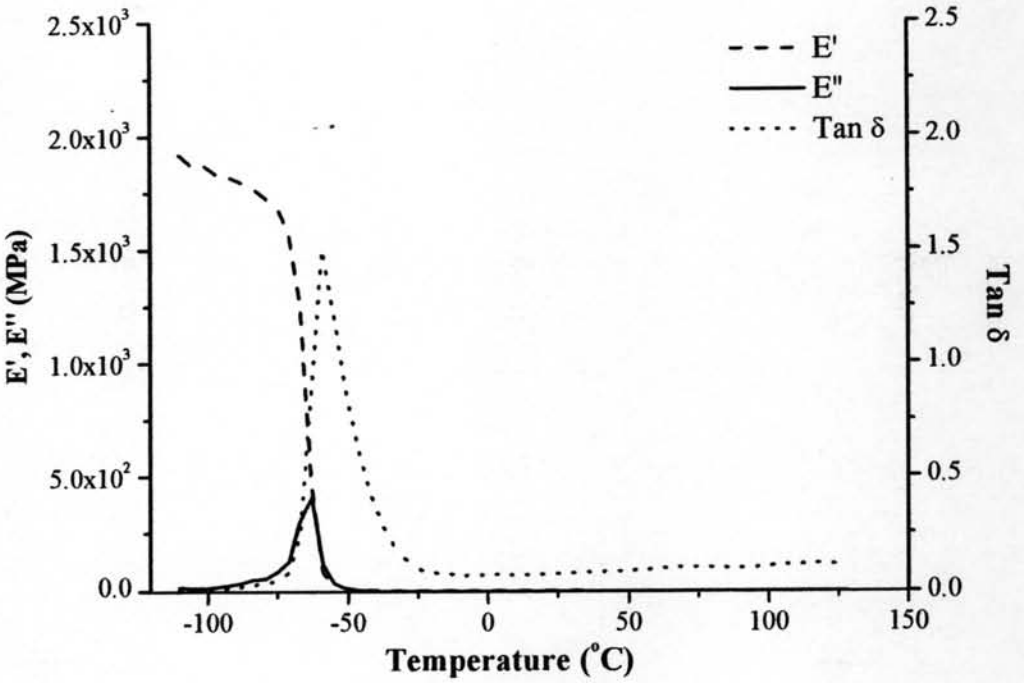

Figure I6 Storage modulus, loss modulus and tan δ of A50,3-1.

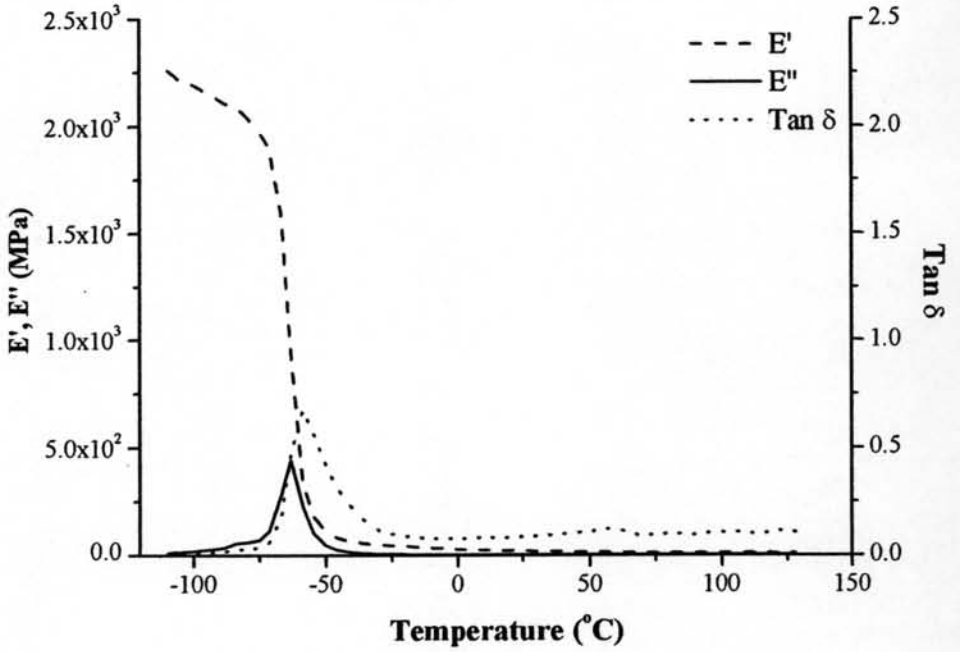

Figure I7 Storage modulus, loss modulus and tan δ of A100,1-1.

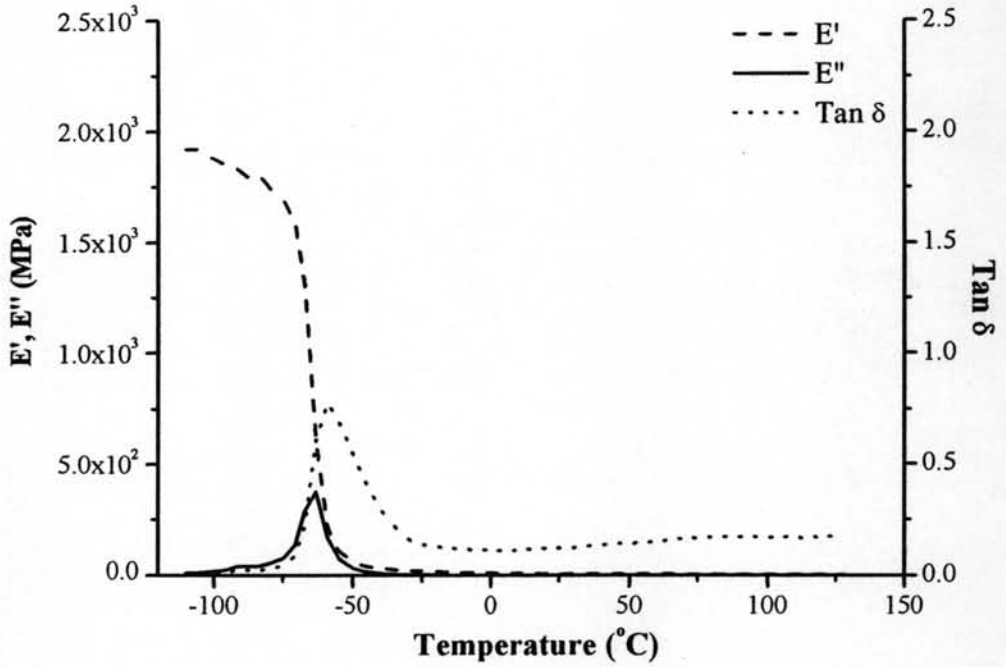

Figure I8 Storage modulus, loss modulus and tan δ of A100,2-1.

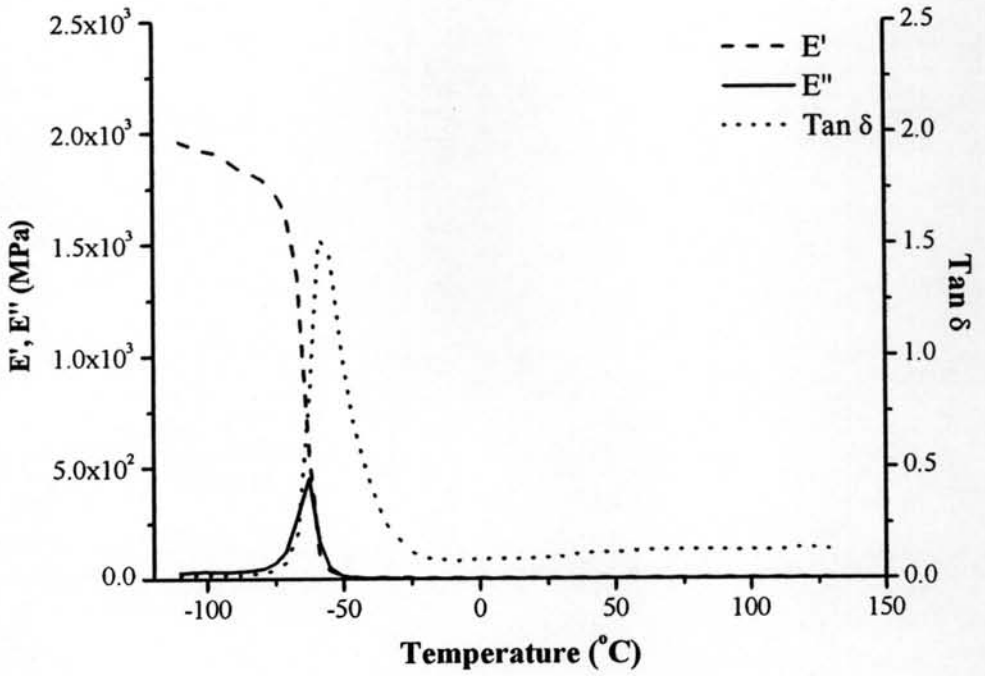

Figure I9 Storage modulus, loss modulus and tan δ of A100,3-1.

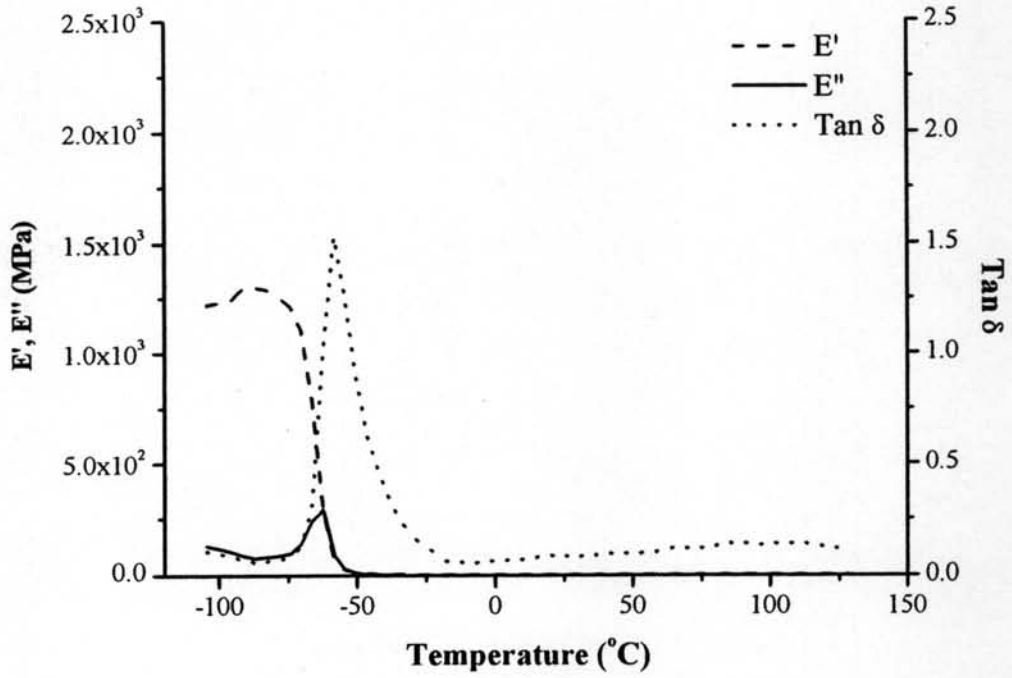

Figure I10 Storage modulus, loss modulus and tan δ of B20,1-1.

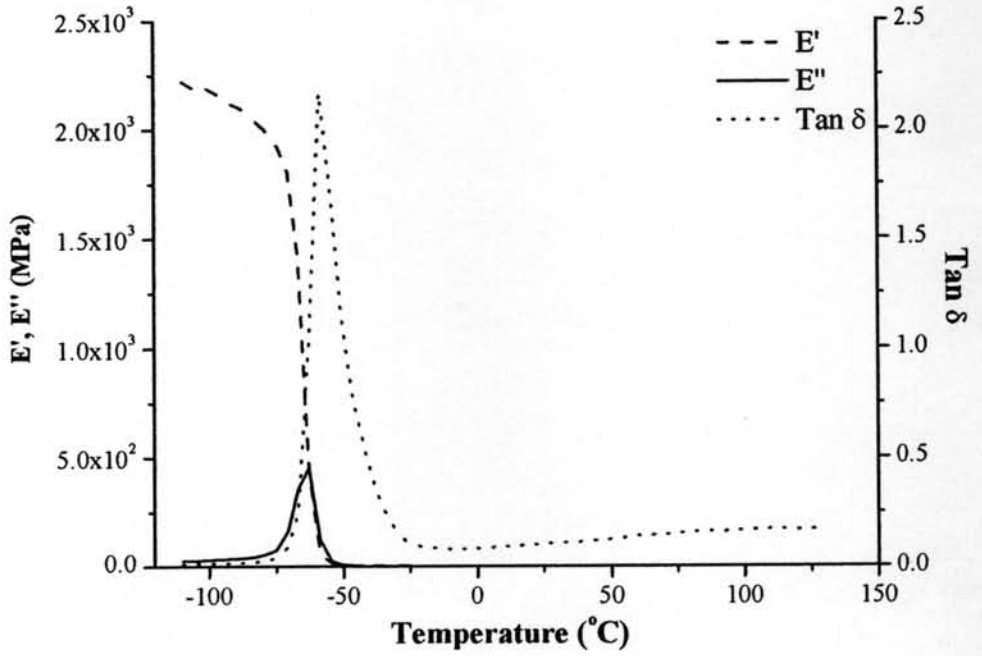

Figure I11 Storage modulus, loss modulus and tan δ of B20,2-1.

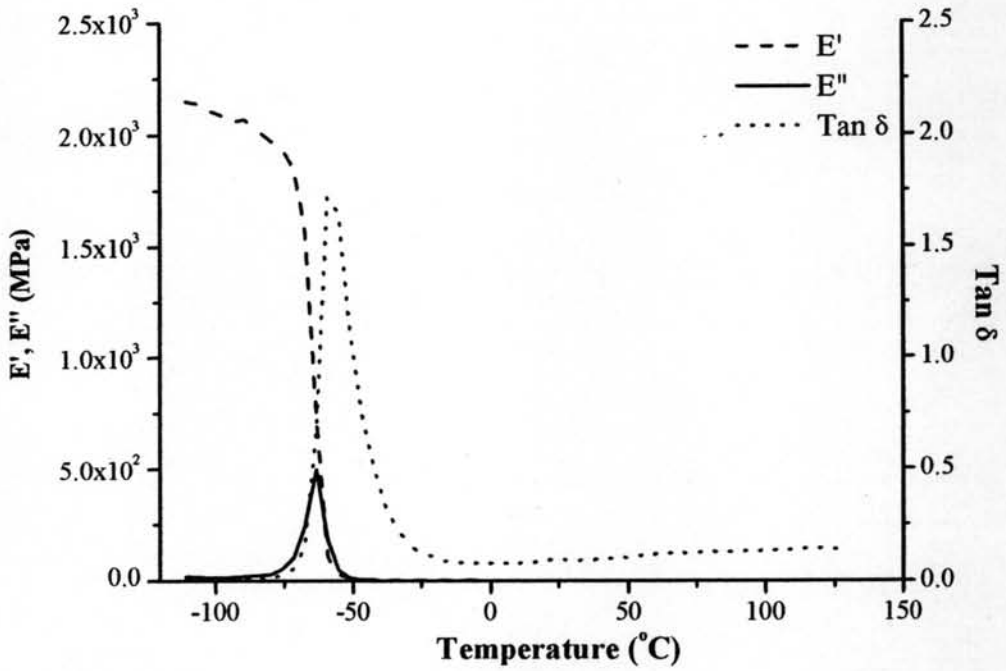

Figure I12 Storage modulus, loss modulus and tan δ of B20,3-1.

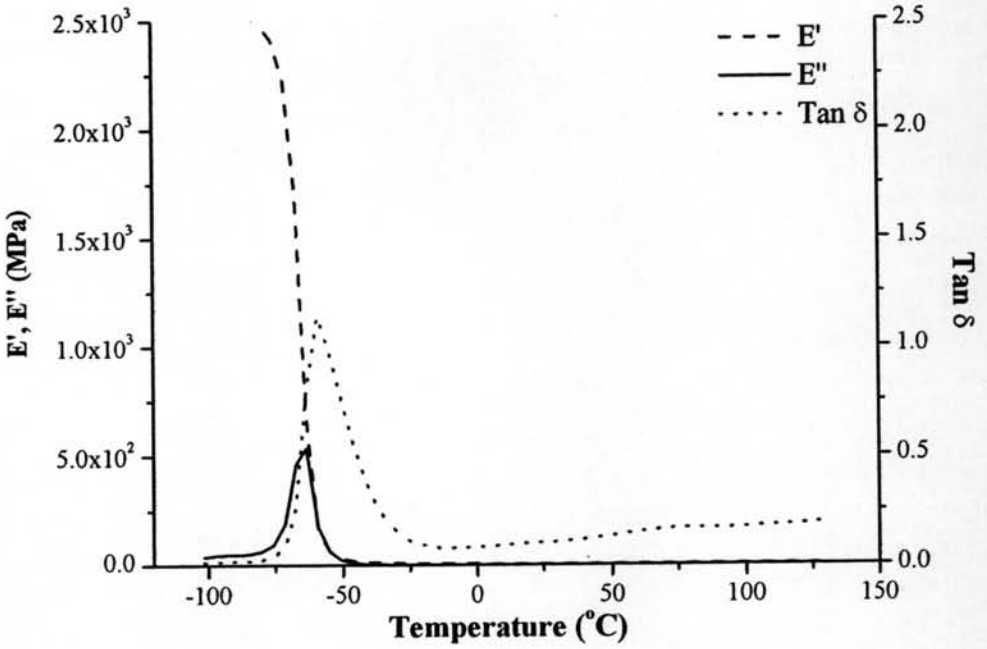

Figure I13 Storage modulus, loss modulus and tan δ of B50,1-1.

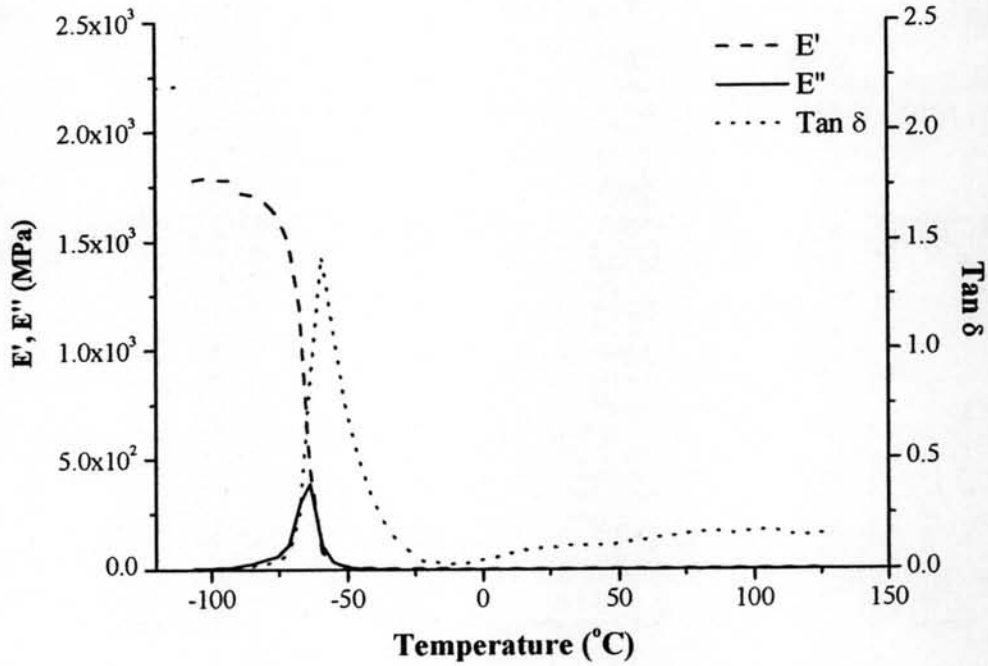

Figure I14 Storage modulus, loss modulus and tan δ of B50,2-1.

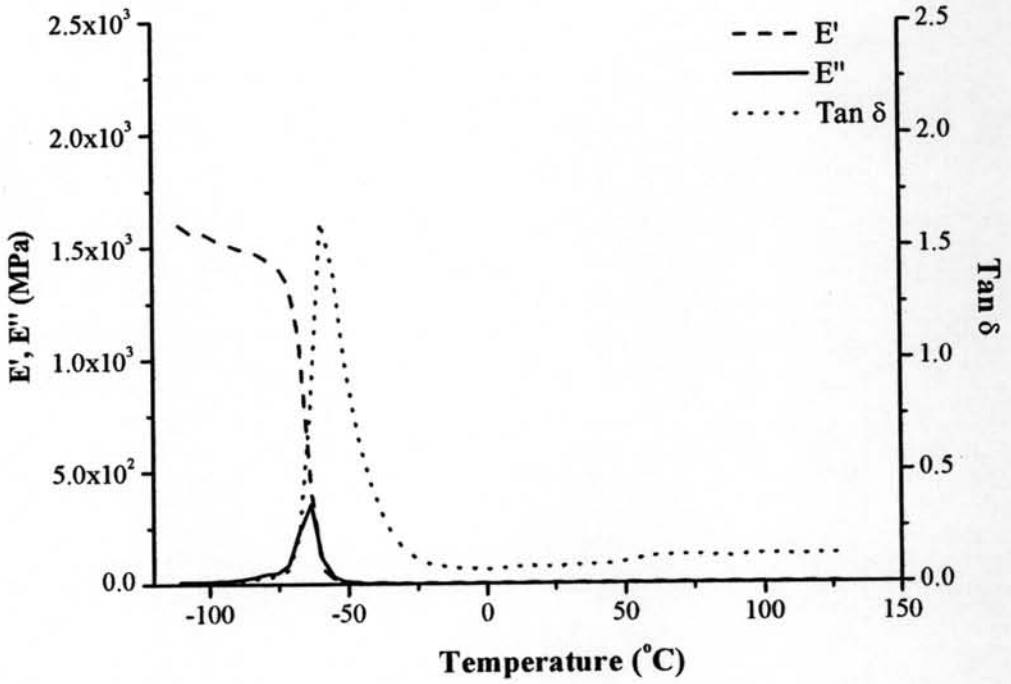

Figure I15 Storage modulus, loss modulus and tan δ of B50,3-1.

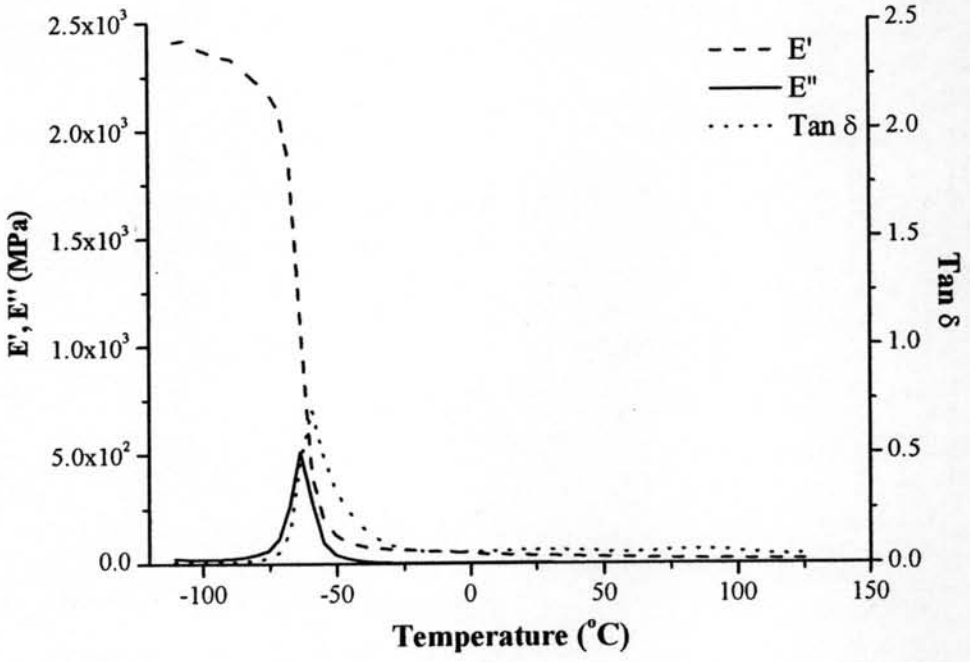

Figure I16 Storage modulus, loss modulus and tan δ of B100,1-1.

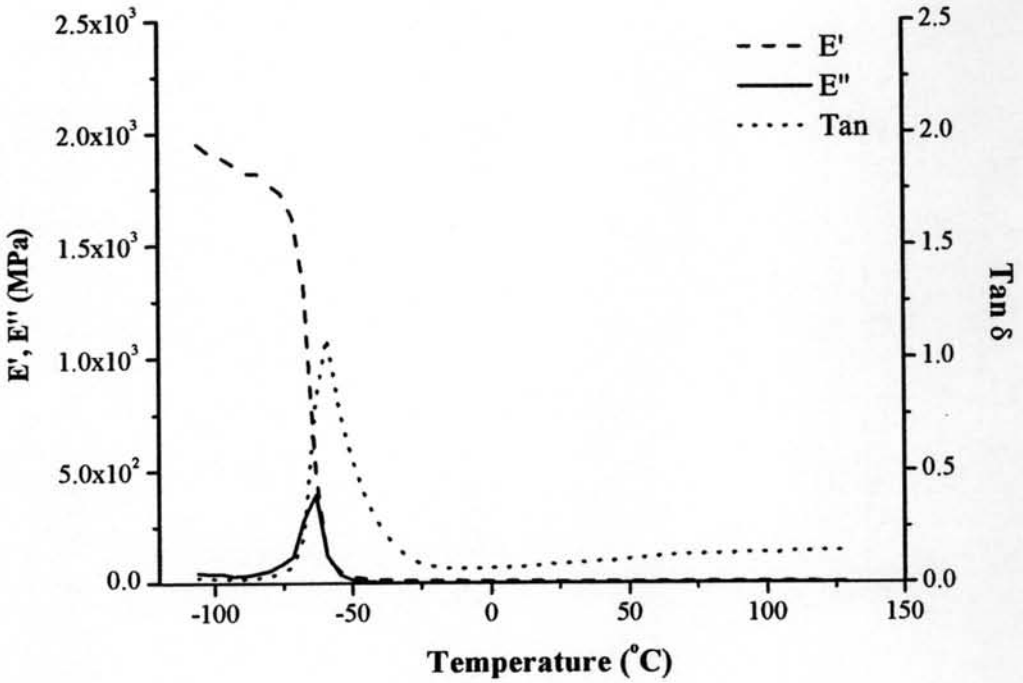

Figure I17 Storage modulus, loss modulus and tan δ of B100,2-1.

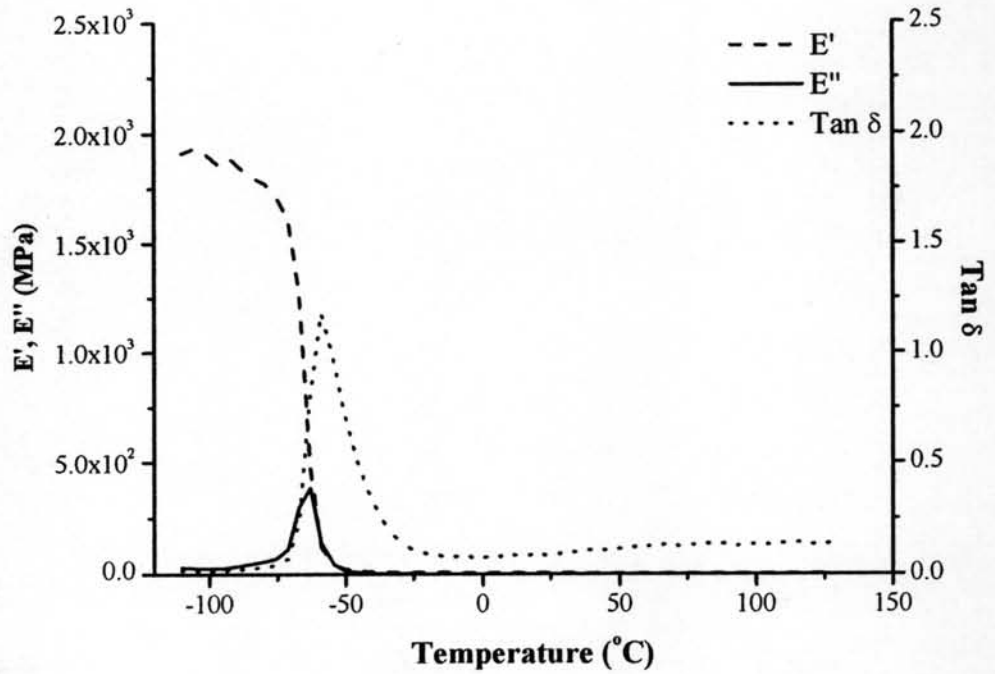

Figure I18 Storage modulus, loss modulus and tan δ of B100,3-1.

Appendix J Data of Conductivity Measurement

Table J1 Volume and surface conductivity of the admicelled rubbers

Sample	Thickness (cm)	Volume conductivity (S/cm)	Surface conductivity (S)
A20,1-1	0.08892	1.9E-08	6.3E-08
A20,2-1	0.03258	2.9E-08	4.1E-08
A20,3-1	0.04417	4.6E-10	3.1E-08
A50,1-1	0.02646	1.6E-06	1.1E-07
A50,2-1	0.02760	2.9E-07	5.5E-08
A50,3-1	0.07083	4.5E-09	1.5E-08
A100,1-1	0.05933	1.0E-05	9.6E-07
A100,2-1	0.05980	7.2E-06	2.6E-07
A100,3-1	0.05920	3.3E-06	8.9E-08
B20,1-1	0.03685	8.3E-07	5.9E-07
B20,2-1	0.07557	2.3E-07	1.0E-07
B20,3-1	0.06927	1.6E-07	5.7E-09
B50,1-1	0.04258	4.8E-06	2.2E-06
B50,2-1	0.04091	1.5E-06	4.5E-07
B50,3-1	0.06510	2.6E-06	3.6E-07
B100,1-1	0.03669	5.5E-06	5.8E-07
B100,2-1	0.03871	6.8E-06	1.2E-06
B100,3-1	0.05008	3.9E-06	9.0E-07
C20,1-1	0.08967	2.1E-08	3.2E-09
C20,2-1	0.04467	5.3E-10	2.7E-09
C20,3-1	0.04469	3.1E-09	1.0E-09
C50,1-1	0.04293	5.0E-06	1.3E-07
C50,2-1	0.05425	2.9E-06	2.0E-07

Sample	Thickness (cm)	Volume conductivity (S/cm)	Surface conductivity (S)
C50,3-1	0.05208	3.7E-07	1.5E-08
C100,1-1	0.03375	6.8E-06	2.6E-06
C100,2-1	0.04936	1.6E-06	3.6E-07
C100,3-1	0.07655	6.0E-06	4.7E-07

Note

Ax,y-z:

A,B,C = [NaCl] 0.0, 0.1, 0.3 M, x = [PPy] 20, 50, 100 mM, y-z = [Mo]/[In]

Table J2 Volume conductivity of the stretched admicelled rubbers

Strain (%)	Conductivity (S/cm)				
	B20,1-1	B50,1-1	B100,1-1	B100,2-1	B100,3-1
0.00	1.12E-07	3.22E-04	2.28E-04	1.17E-04	5.25E-05
0.89	6.81E-08	1.19E-04	2.59E-04	2.08E-05	3.30E-05
1.28	4.02E-08	4.19E-05	2.65E-04	2.12E-05	4.88E-05
2.11	-	5.90E-05	9.87E-05	1.20E-05	7.08E-05
3.06	-	4.56E-06	4.09E-05	5.08E-06	5.52E-06

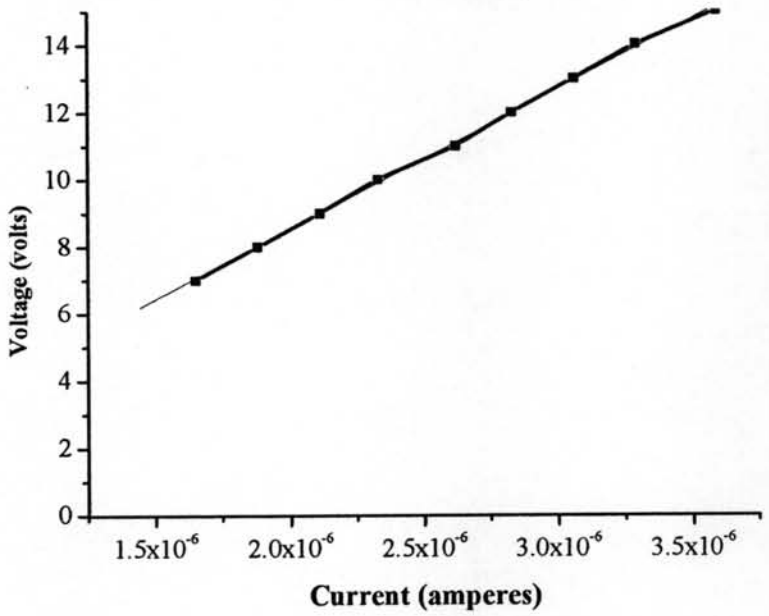

Figure J1 Volume resistance in linear range of A2,3-1.

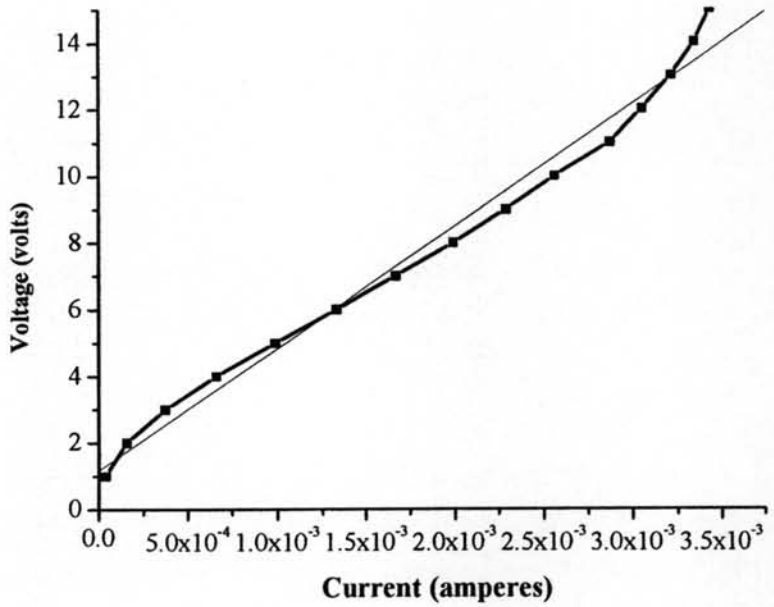

Figure J2 Volume resistance in linear range of A5,2-1.

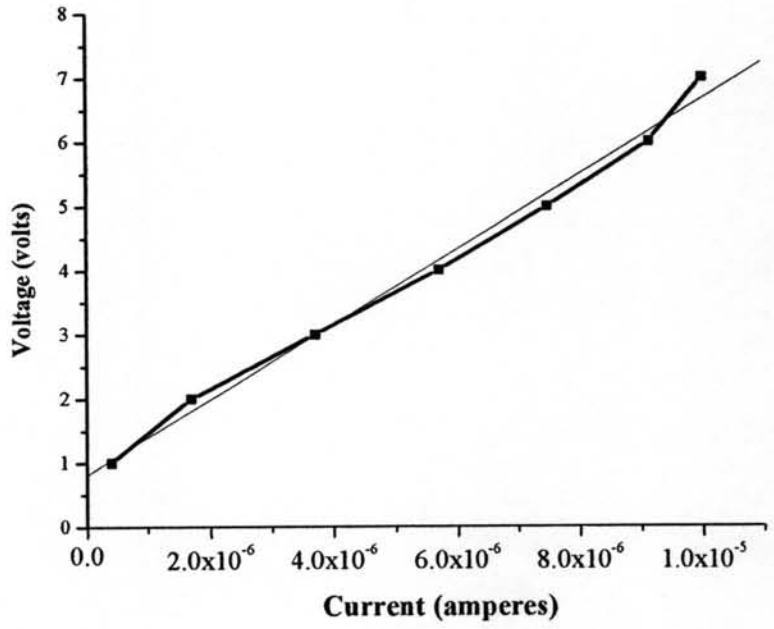

Figure J3 Volume resistance in linear range of A5,3-1.

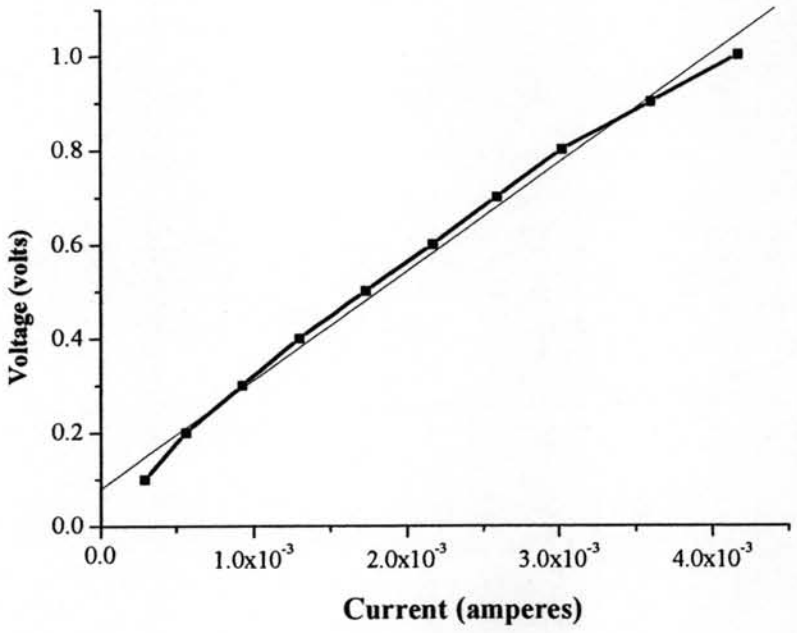

Figure J4 Volume resistance in linear range of A10,1-1.

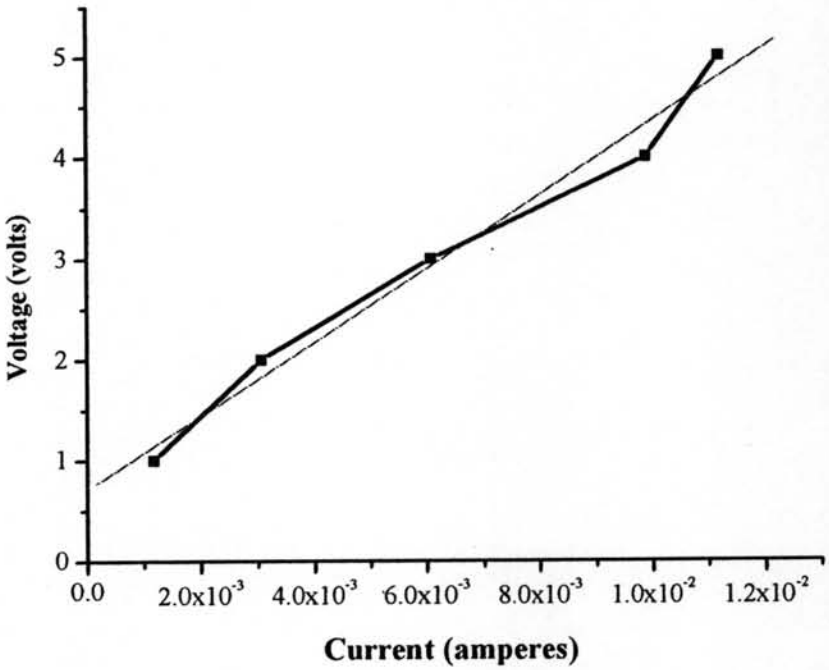

Figure J5 Volume resistance in linear range of A10,2-1.

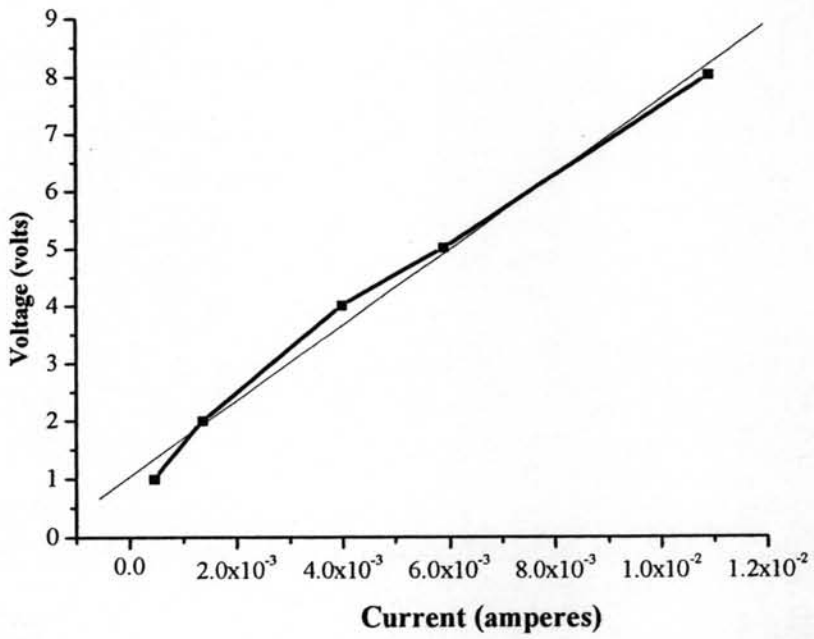

Figure J6 Volume resistance in linear range of A10,3-1.

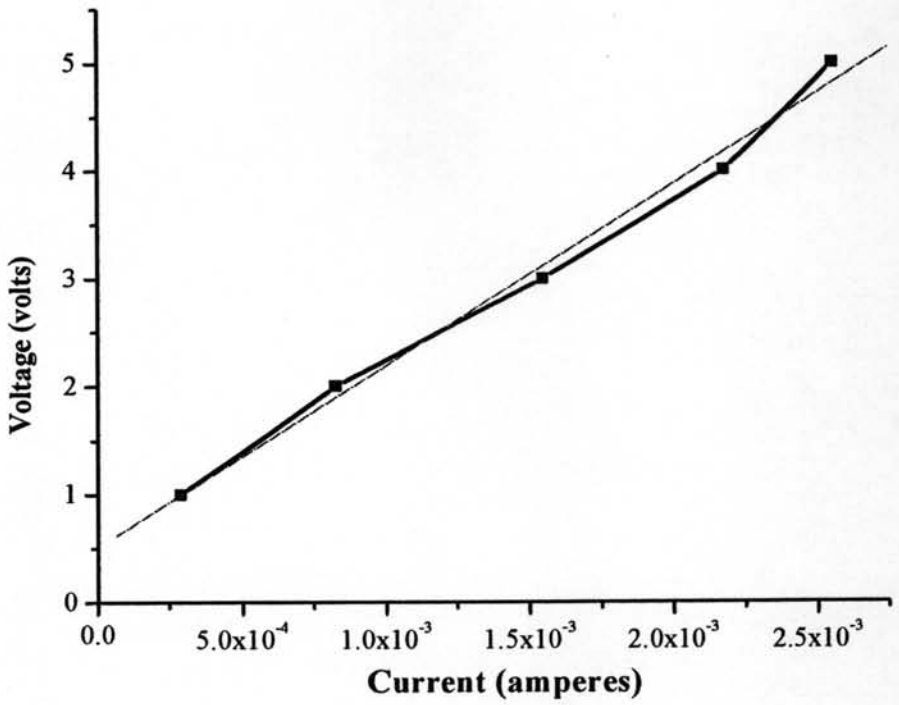

Figure J7 Volume resistance in linear range of B2,1-1.

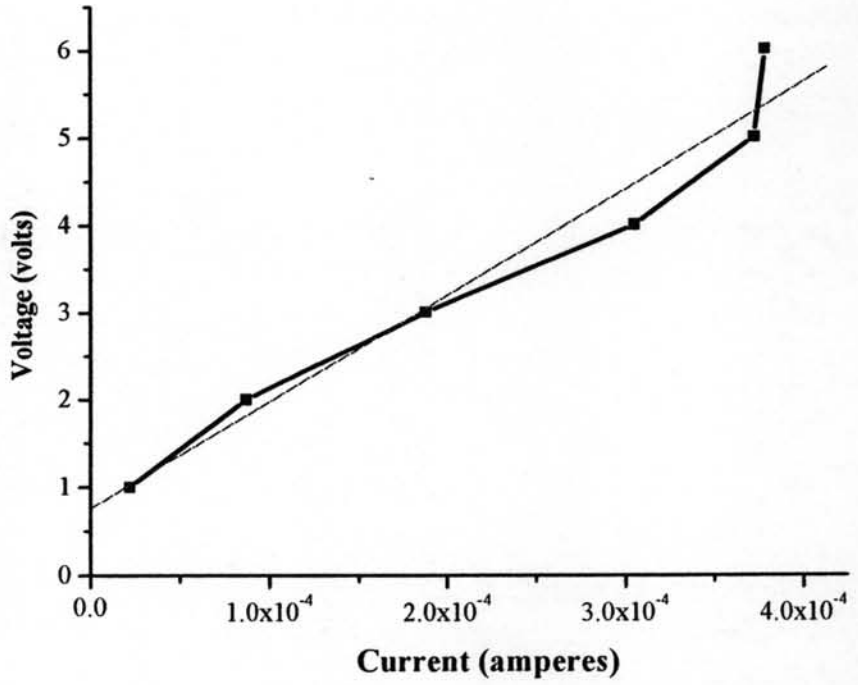

Figure J8 Volume resistance in linear range of B2,2-1.

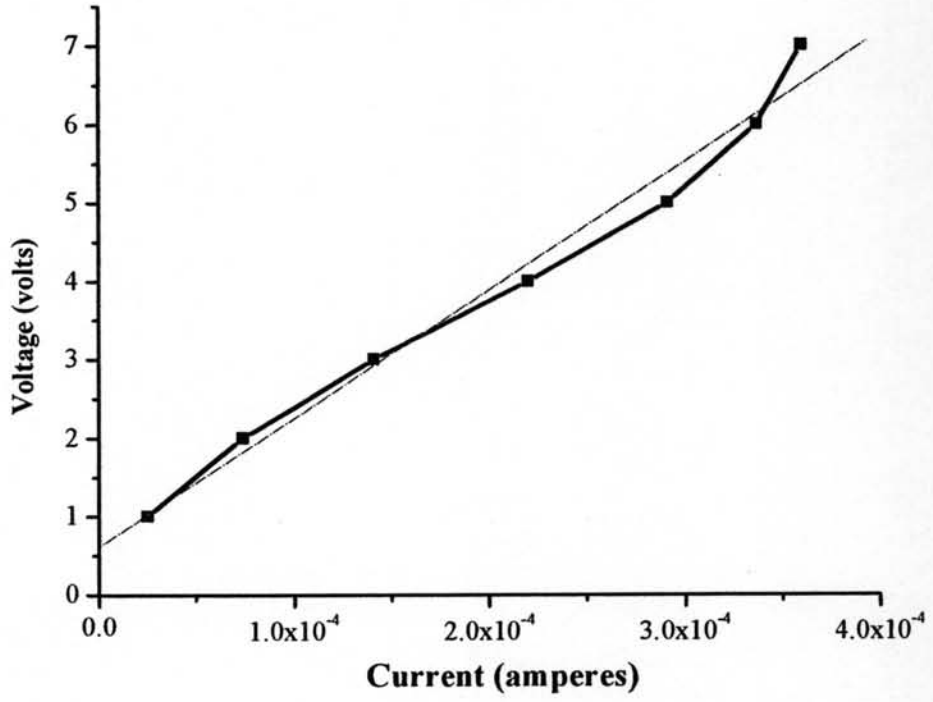

Figure J9 Volume resistance in linear range of B2,3-1.

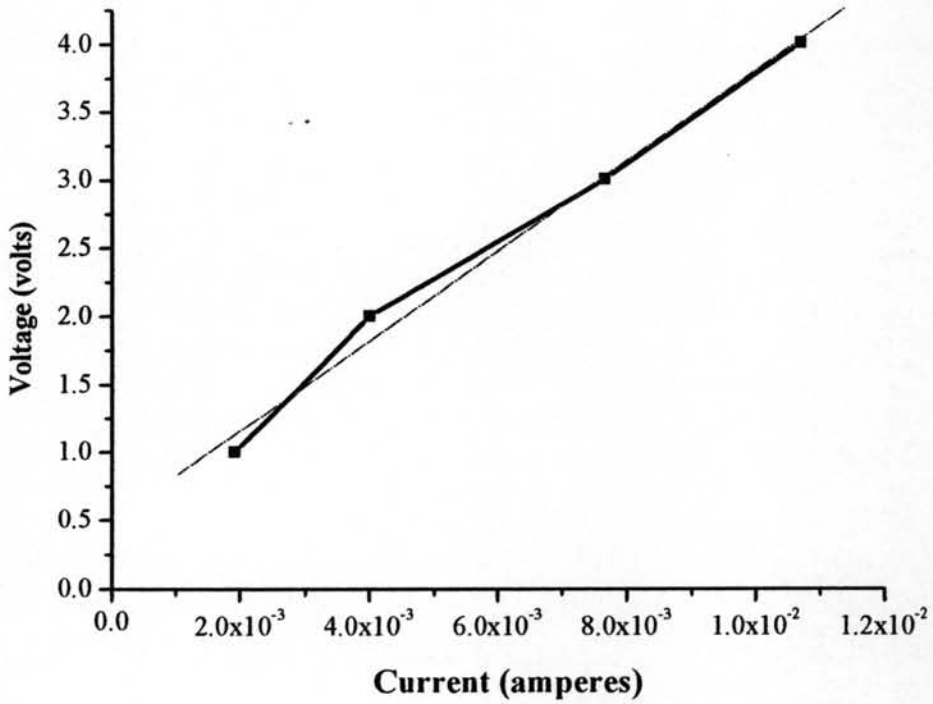

Figure J10 Volume resistance in linear range of B5,1-1.

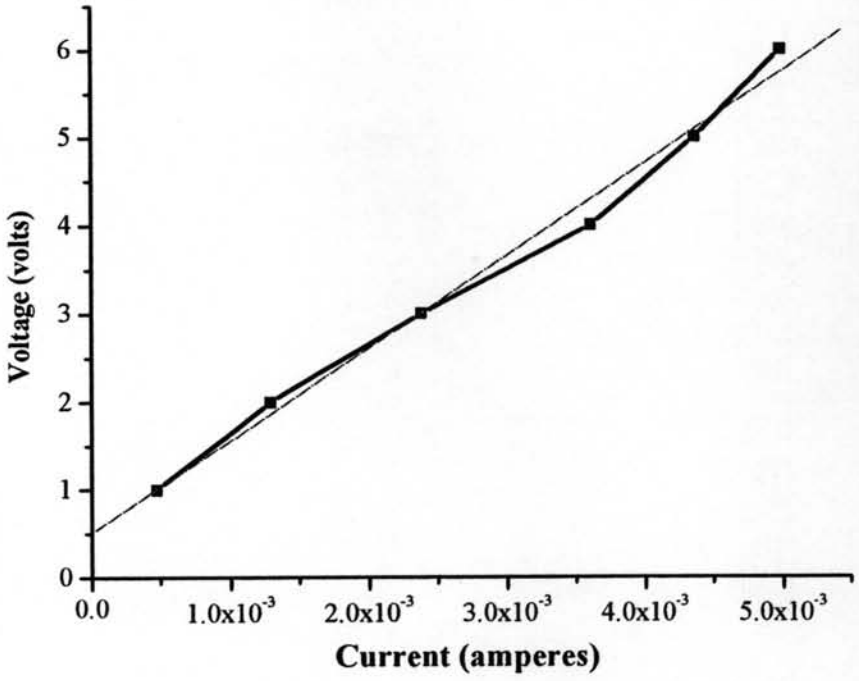

Figure J11 Volume resistance in linear range of B5,2-1.

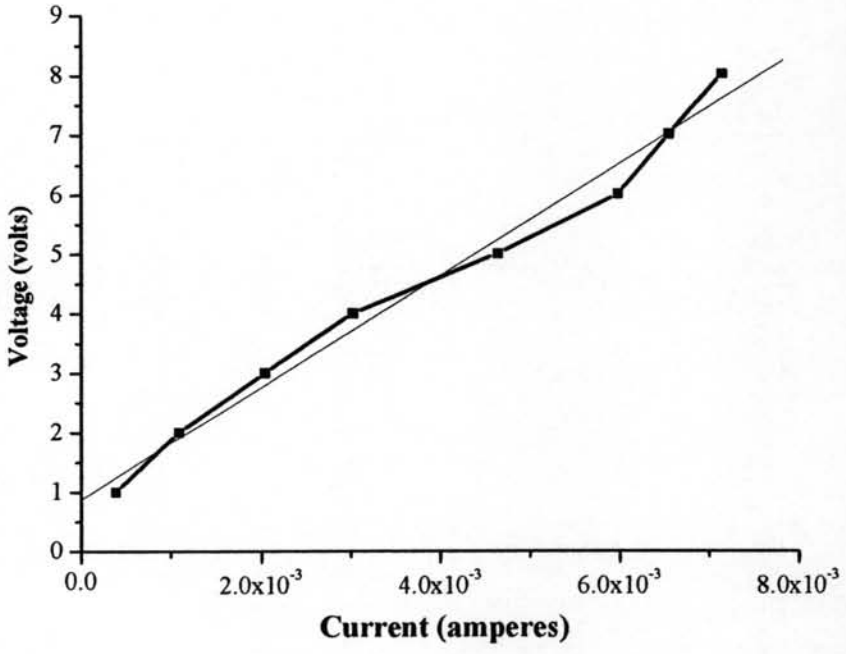

Figure J12 Volume resistance in linear range of B5,3-1.

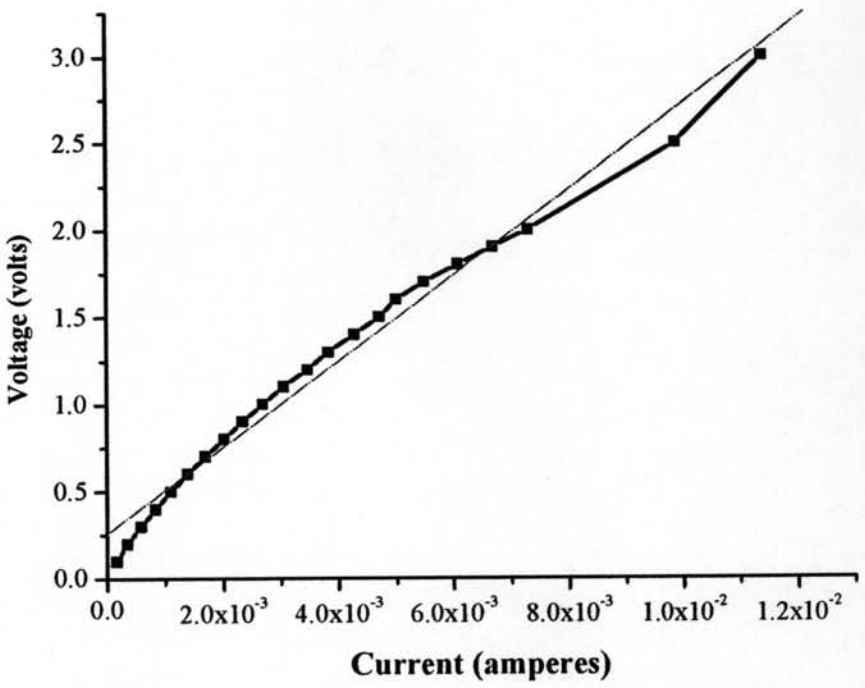

Figure J13 Volume resistance in linear range of B10,1-1.

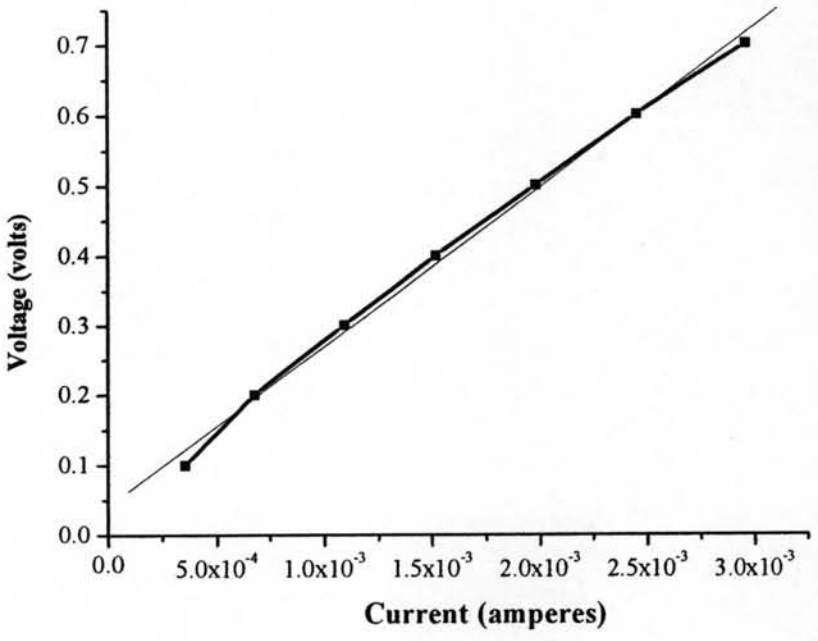

Figure J14 Volume resistance in linear range of B10,2-1.

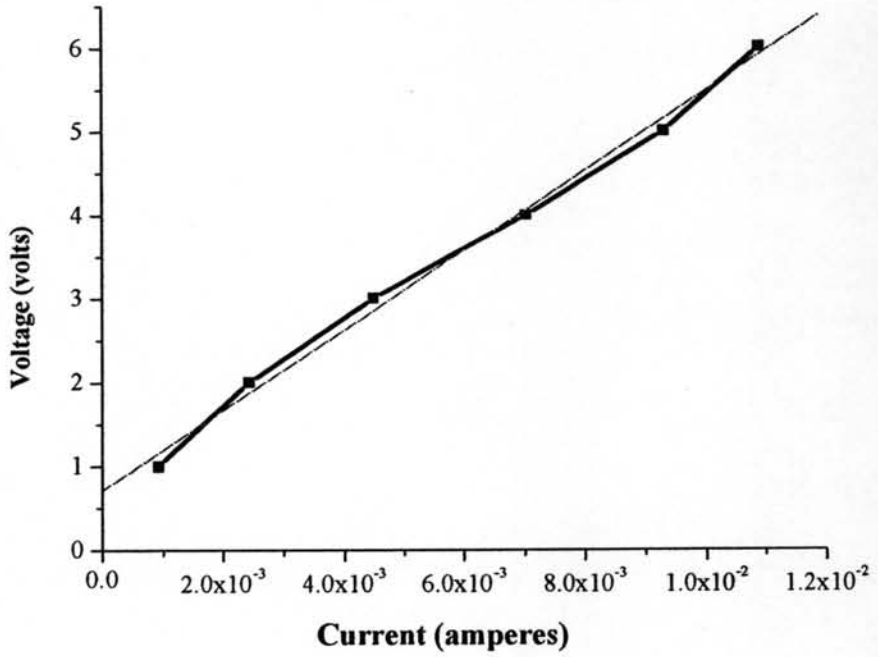

Figure J15 Volume resistance in linear range of B10,3-1.

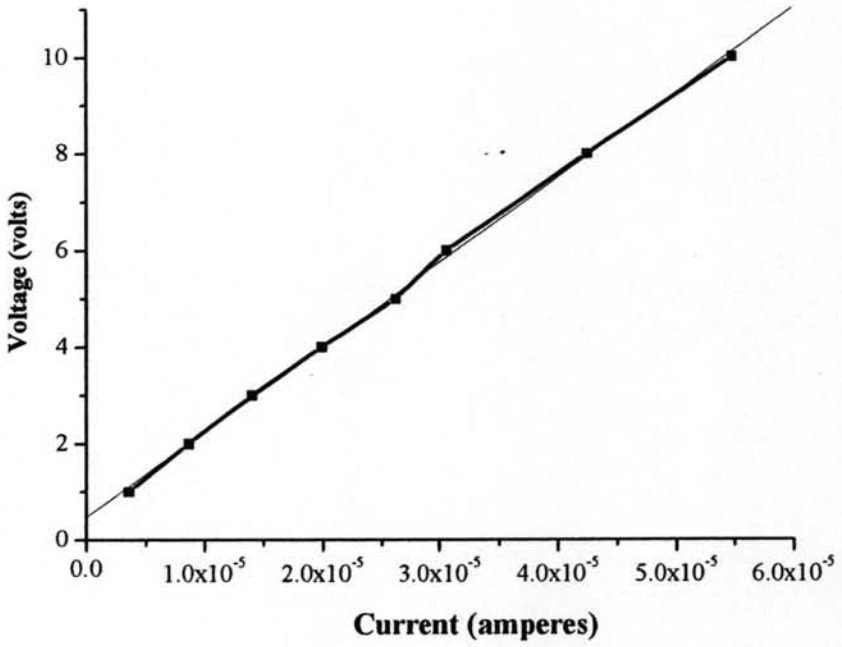

Figure J16 Volume resistance in linear range of C2,1-1.

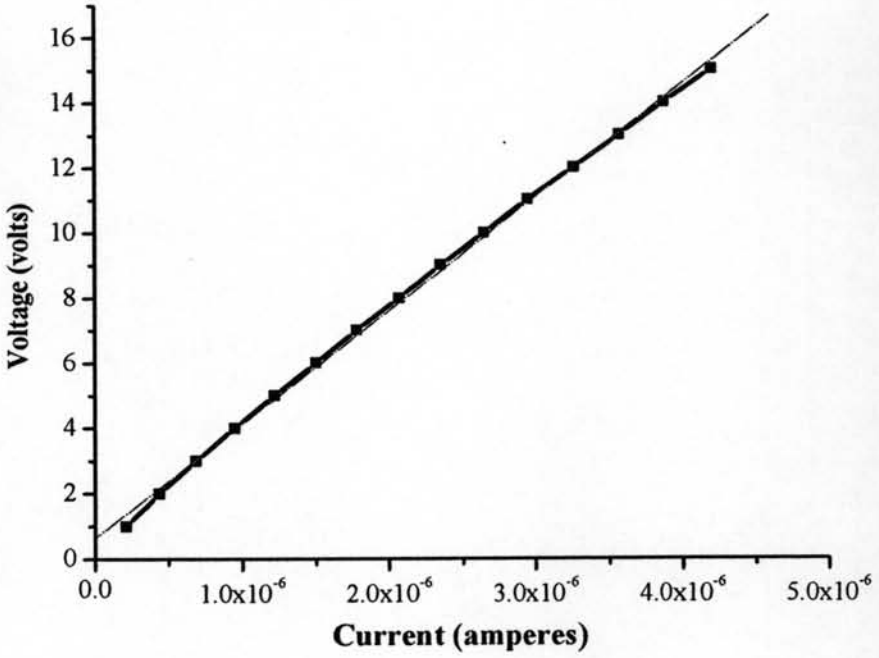

Figure J17 Volume resistance in linear range of C2,2-1.

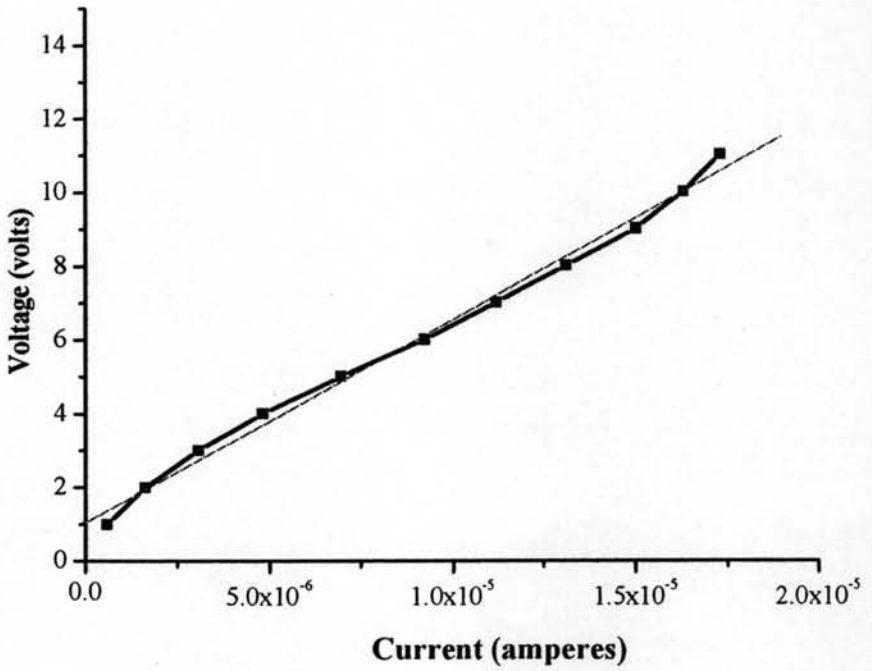

Figure J18 Volume resistance in linear range of C2,3-1.

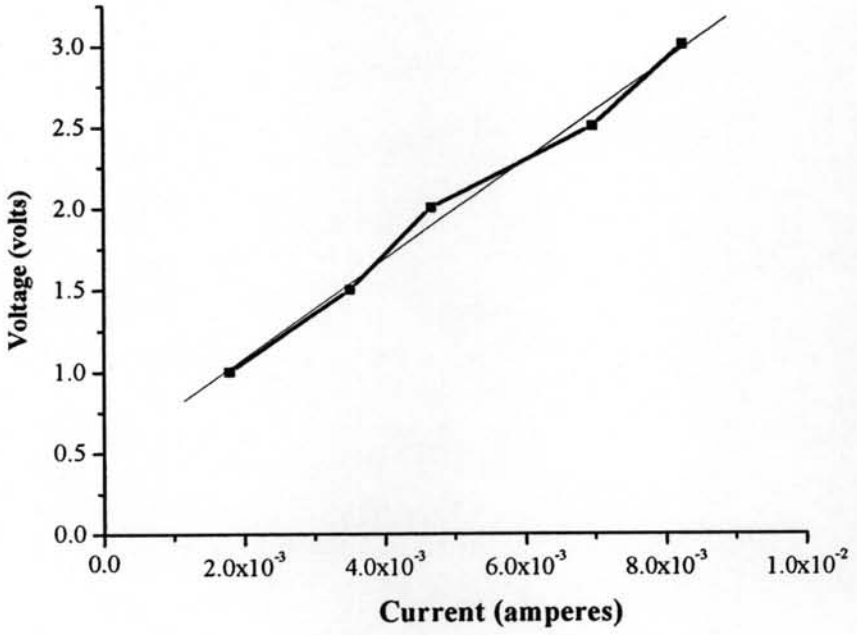

Figure J19 Volume resistance in linear range of C5,1-1.

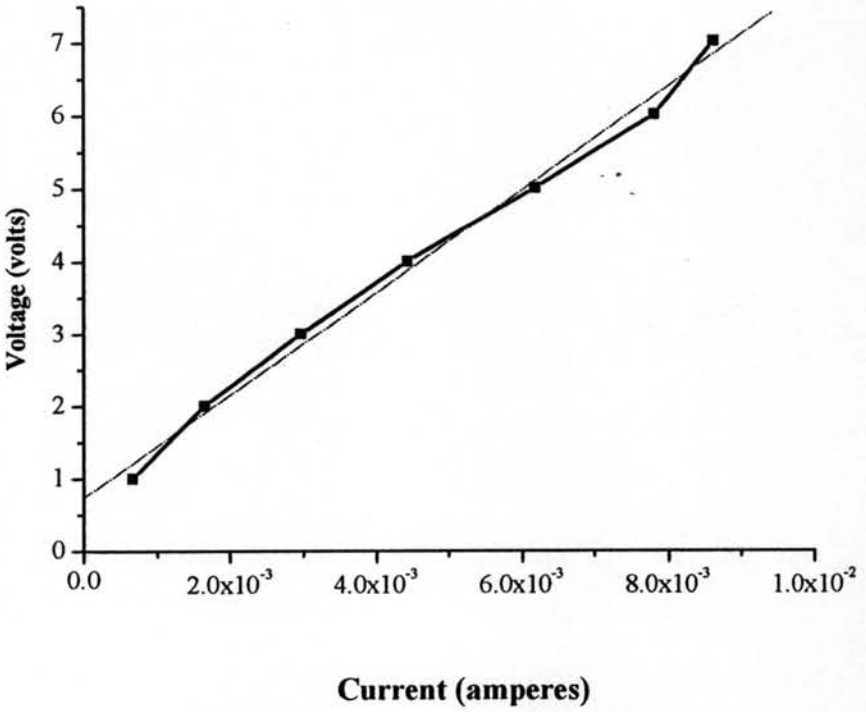

Figure J20 Volume resistance in linear range of C5,2-1.

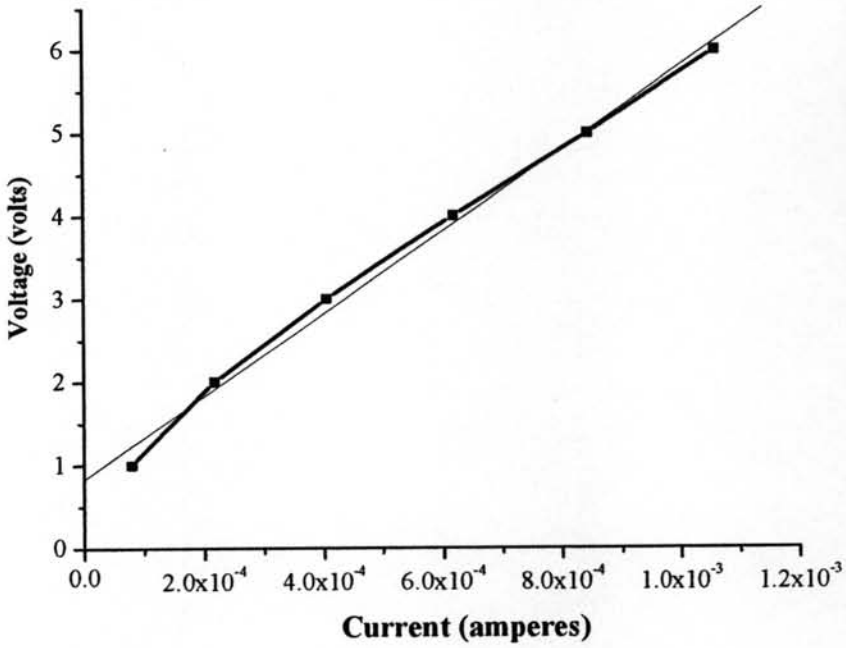

Figure J21 Volume resistance in linear range of C5,3-1.

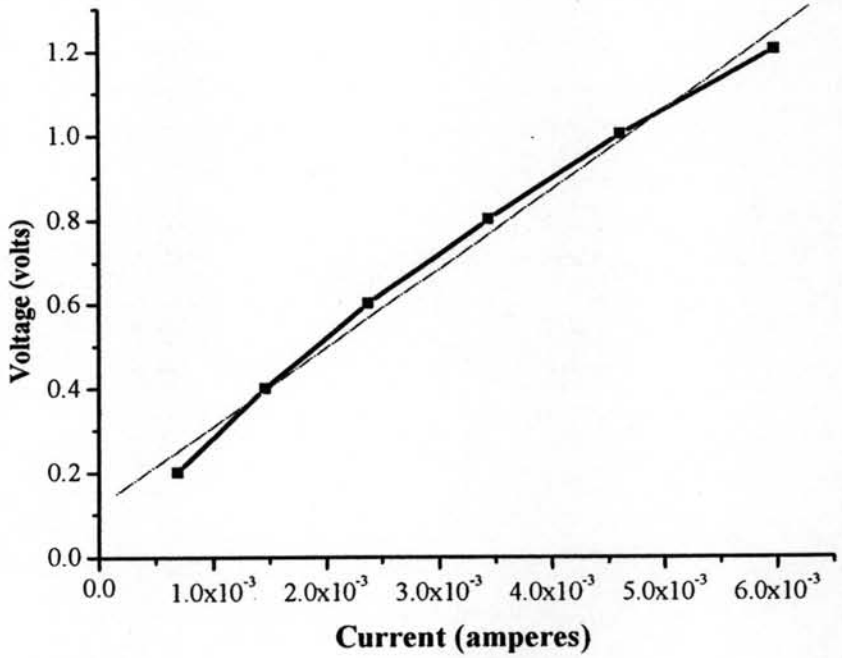

Figure J22 Volume resistance in linear range of C10,1-1.

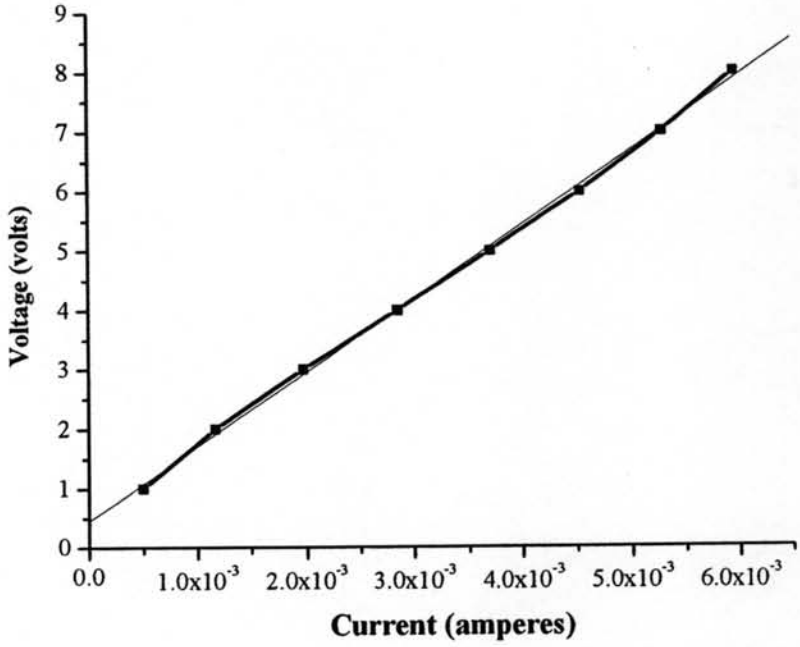

Figure J23 Volume resistance in linear range of C10,2-1.

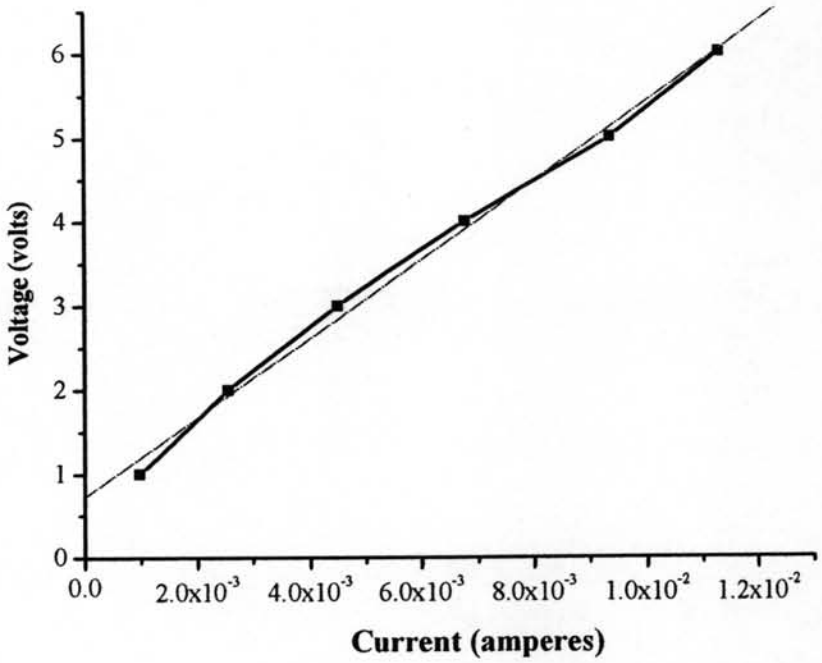

Figure J24 Volume resistance in linear range of C10,3-1.

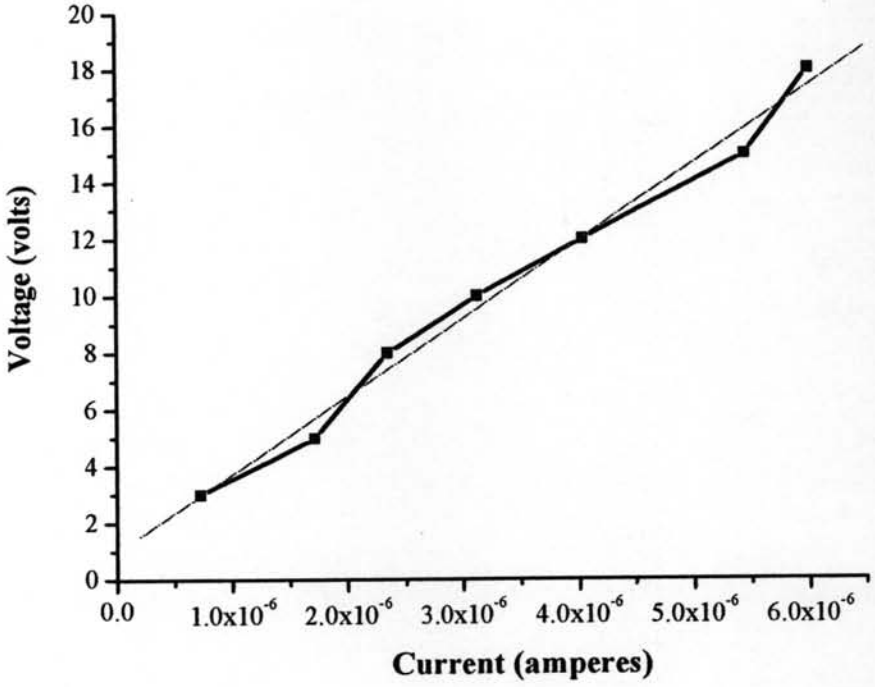

Figure J25 Surface resistance in linear range of A2,1-1.

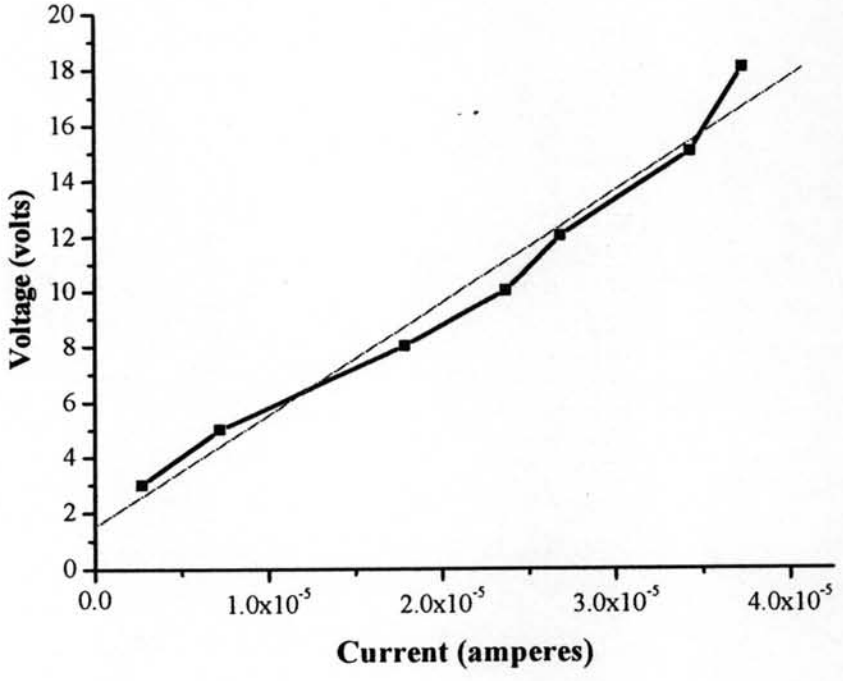

Figure J26 Surface resistance in linear range of A2,2-1.

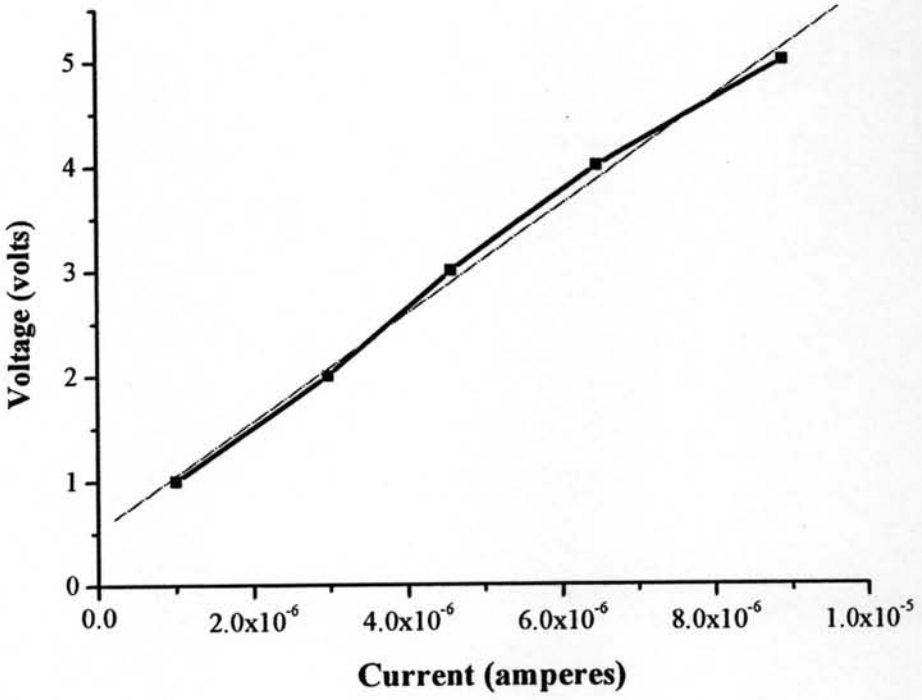

Figure J27 Surface resistance in linear range of A2,3-1.

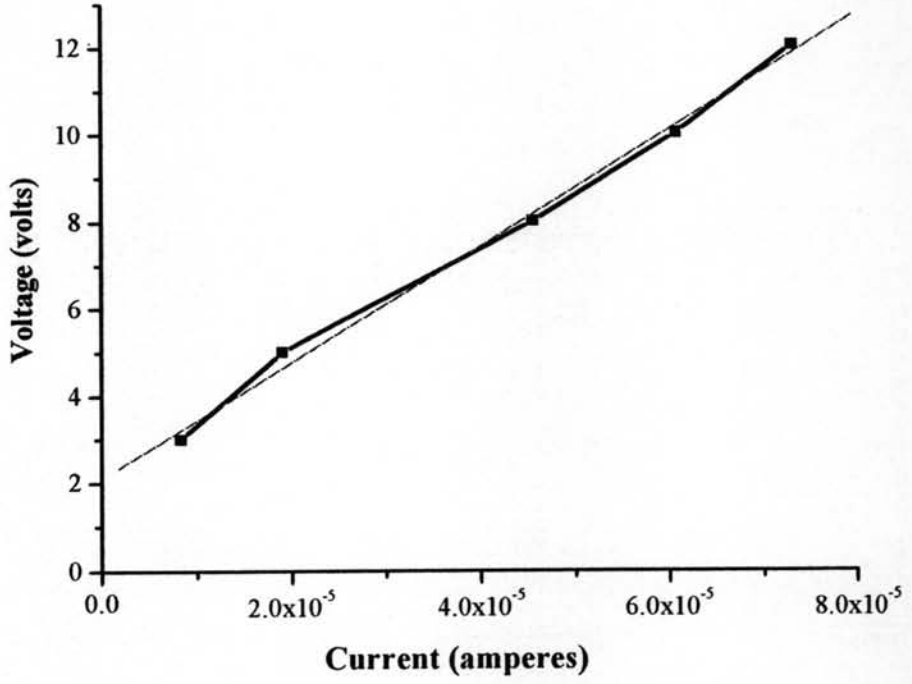

Figure J28 Surface resistance in linear range of A5,1-1.

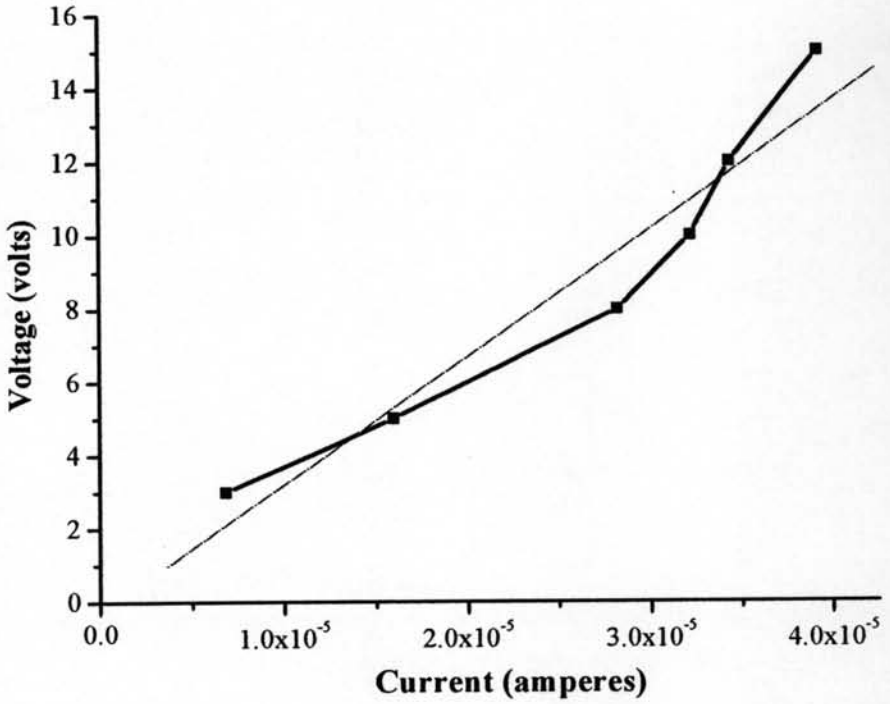

Figure J29 Surface resistance in linear range of A5,2-1.

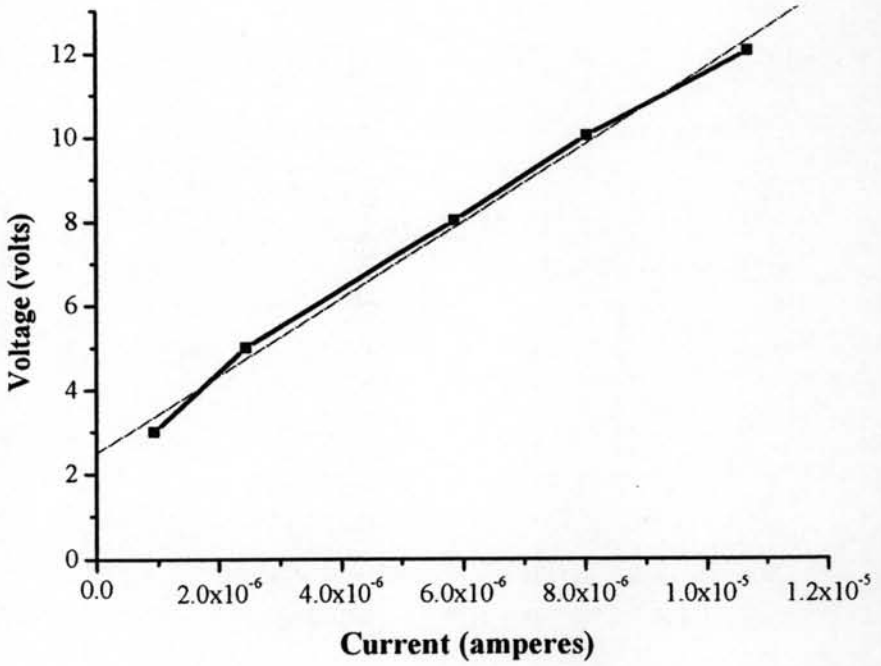

Figure J30 Surface resistance in linear range of A5,3-1.

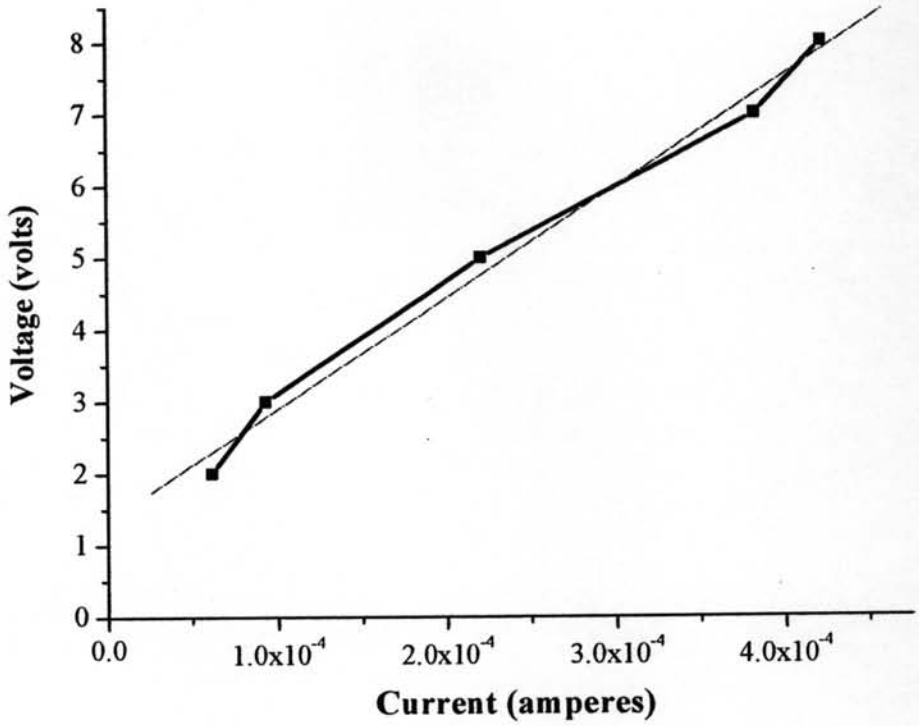

Figure J31 Surface resistance in linear range of A10,1-1.

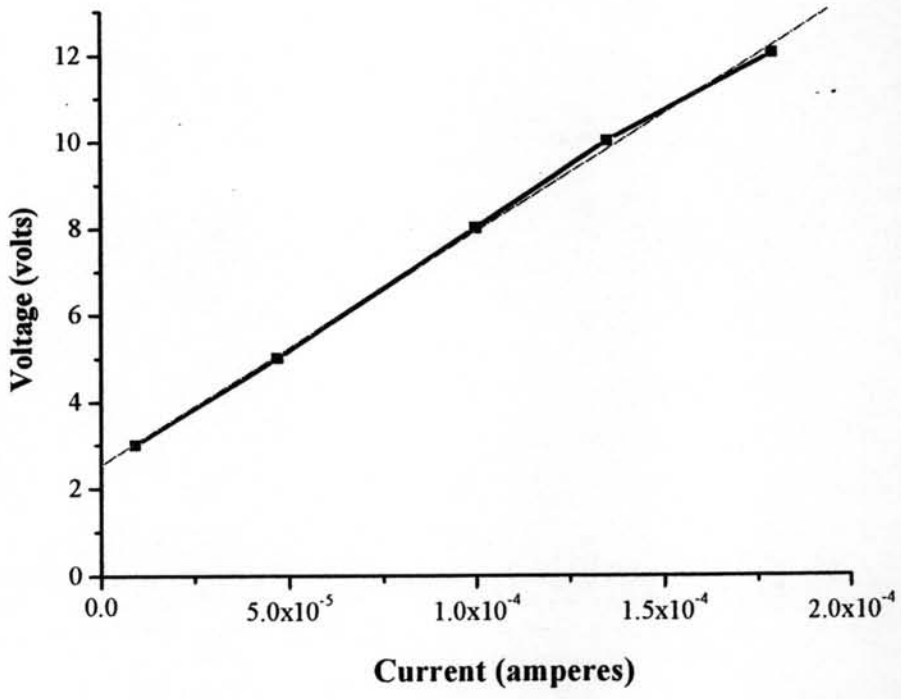

Figure J32 Surface resistance in linear range of A10,2-1.

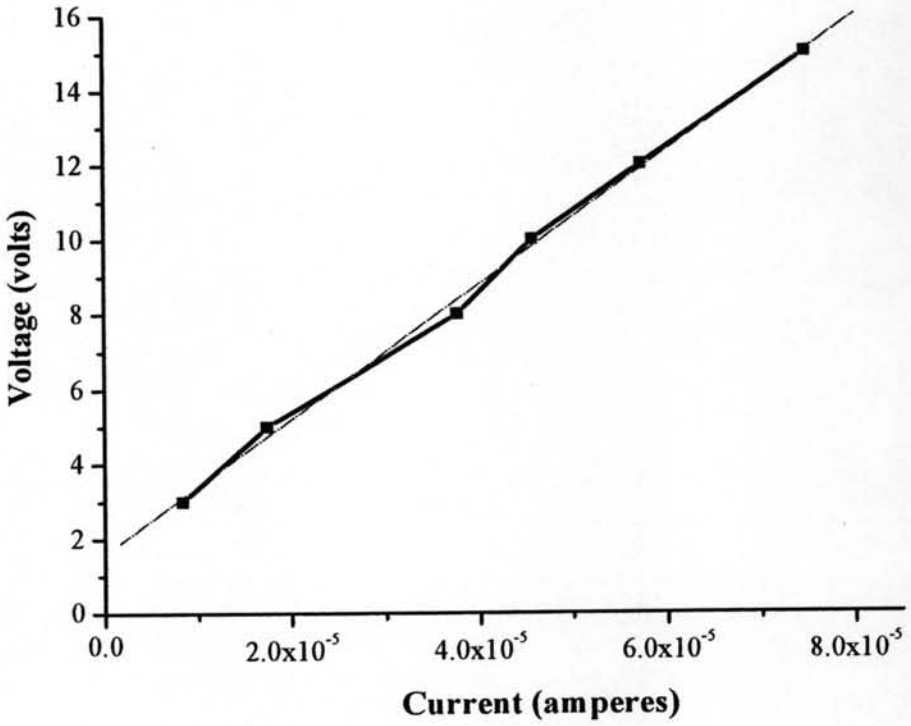

Figure J33 Surface resistance in linear range of A10,3-1.

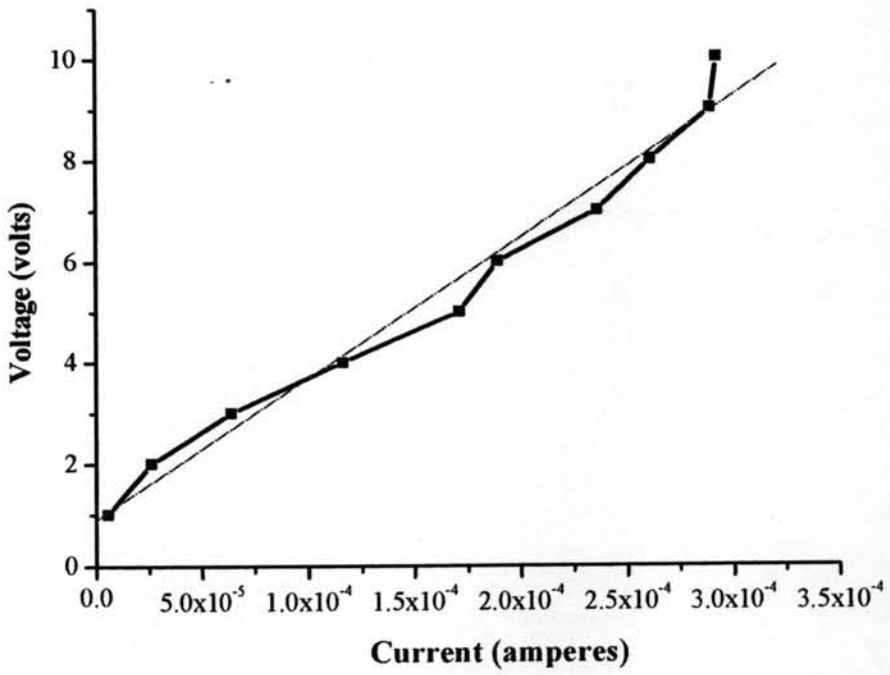

Figure J34 Surface resistance in linear range of B2,1-1.

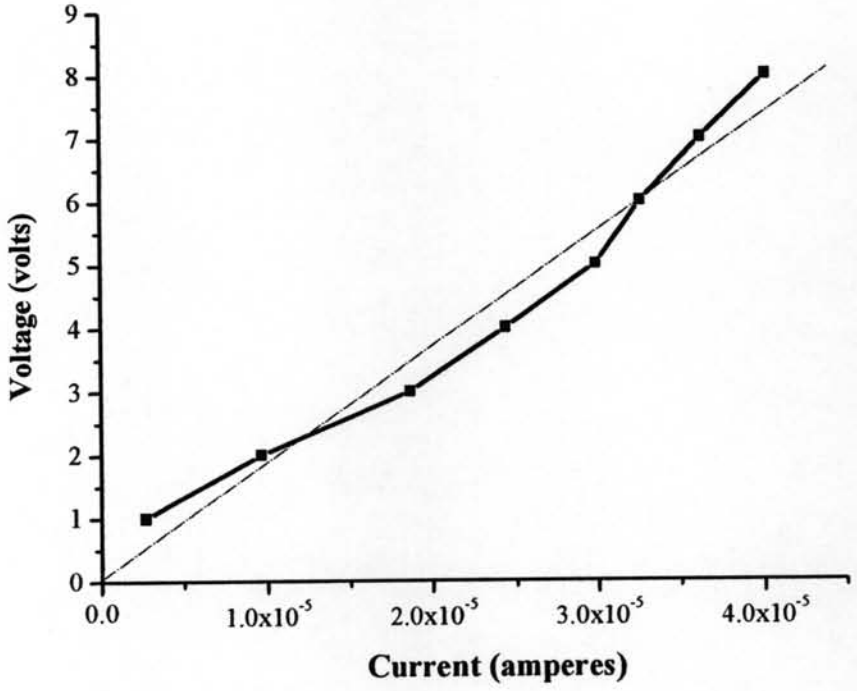

Figure J35 Surface resistance in linear range of B2,2-1.

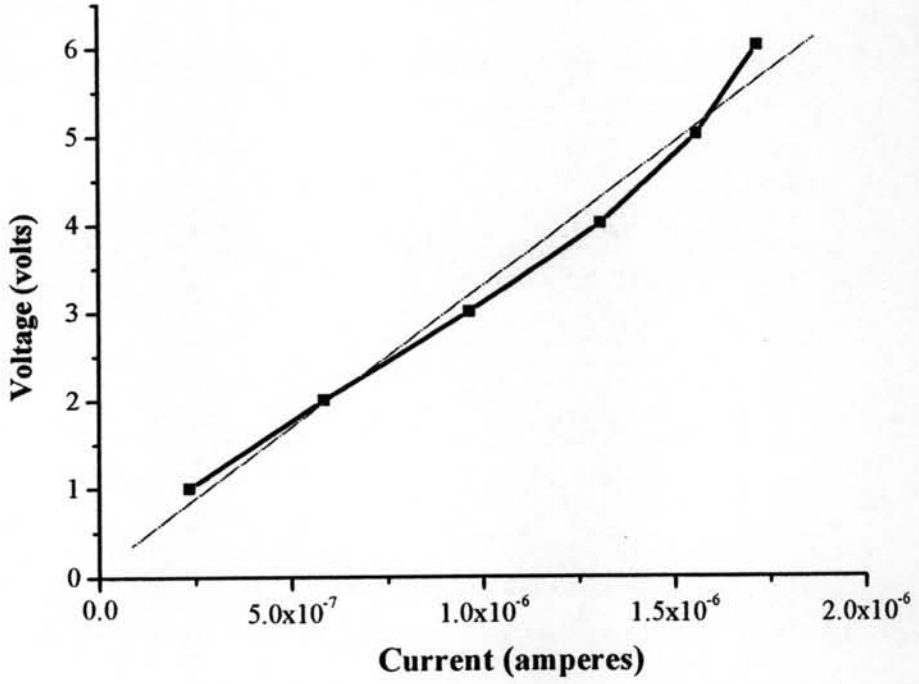

Figure J36 Surface resistance in linear range of B2,3-1.

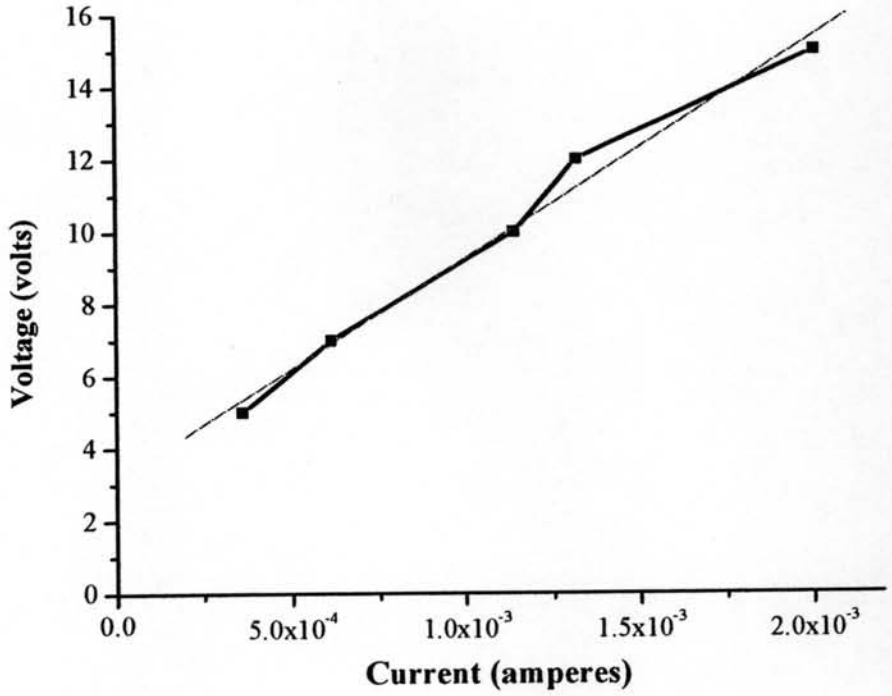

Figure J37 Surface resistance in linear range of B5,1-1.

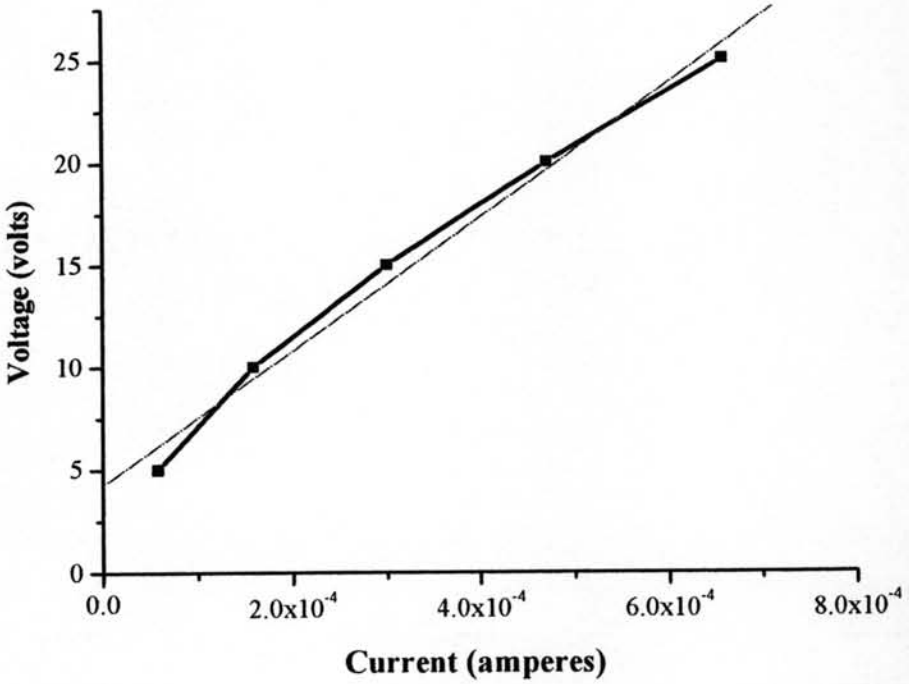

Figure J38 Surface resistance in linear range of B5,2-1.

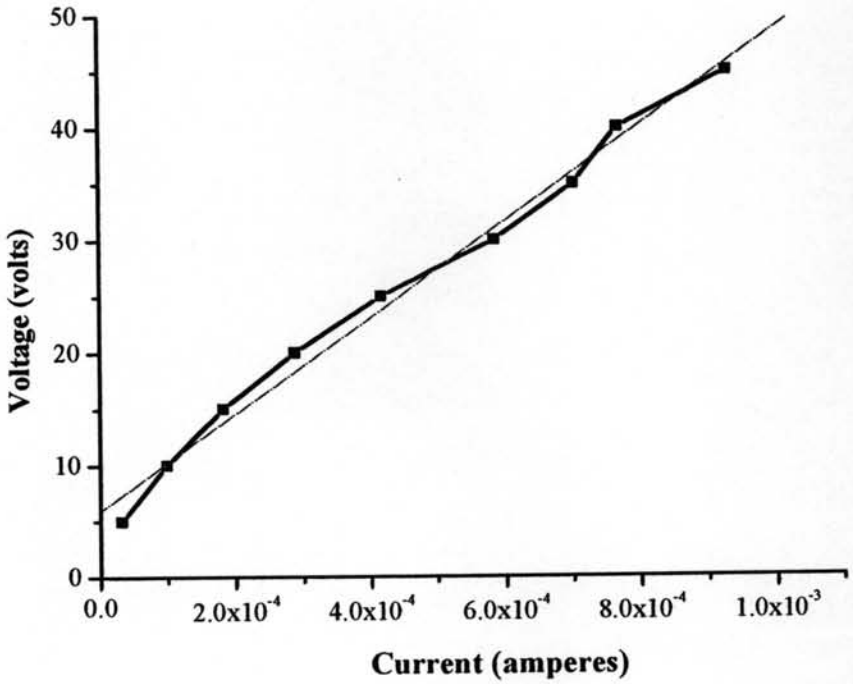

Figure J39 Surface resistance in linear range of B5,3-1.

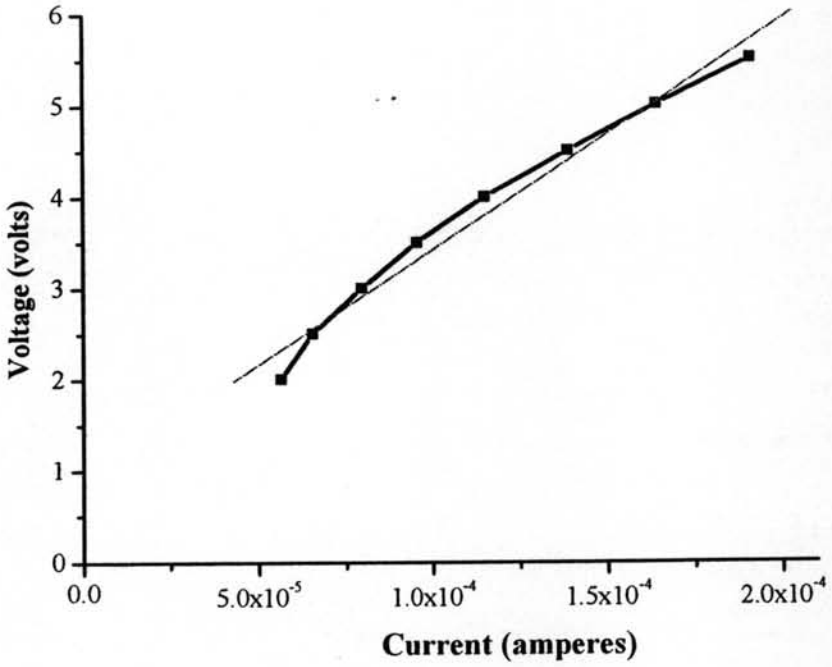

Figure J40 Surface resistance in linear range of B10,1-1.

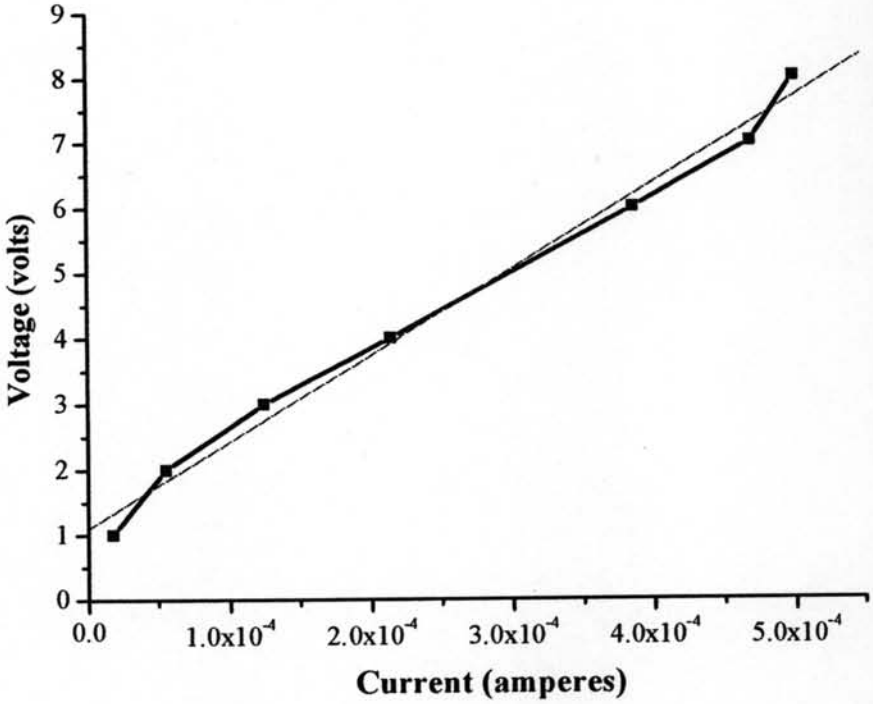

Figure J41 Surface resistance in linear range of B10,2-1.

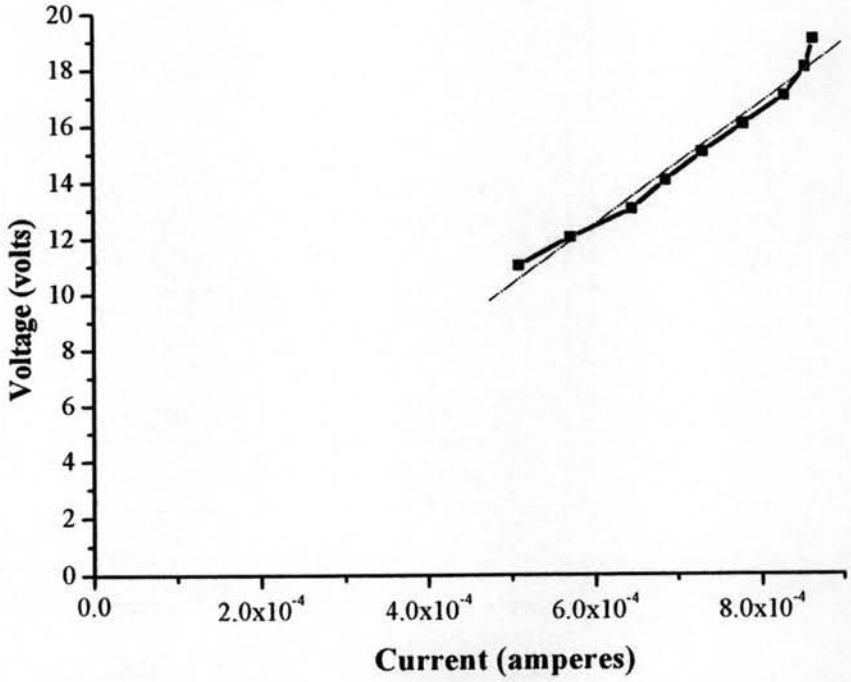

Figure J42 Surface resistance in linear range of B10,3-1.

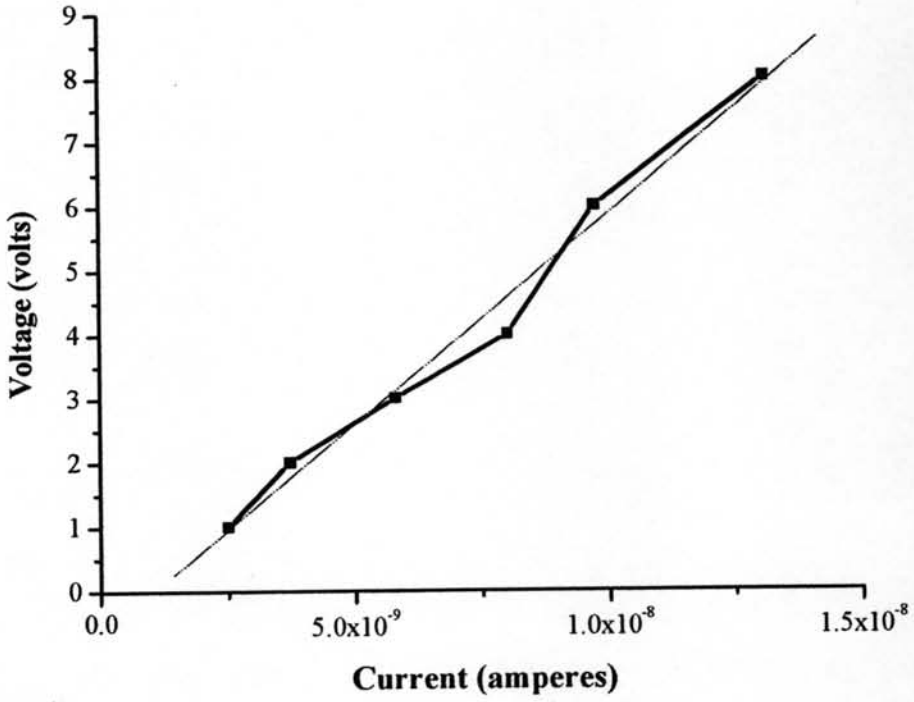

Figure J43 Surface resistance in linear range of C2,1-1.

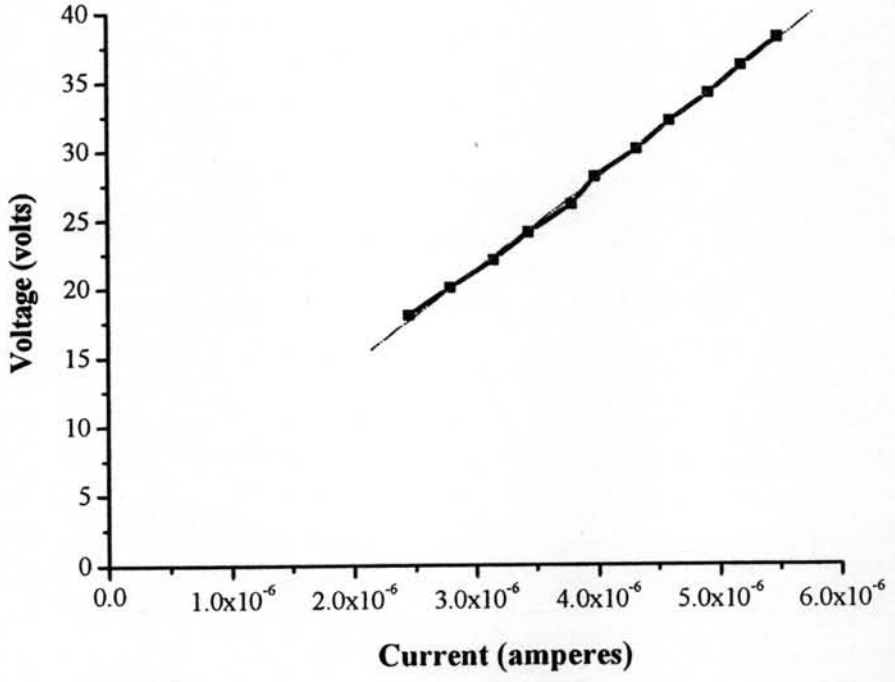

Figure J44 Surface resistance in linear range of C2,2-1.

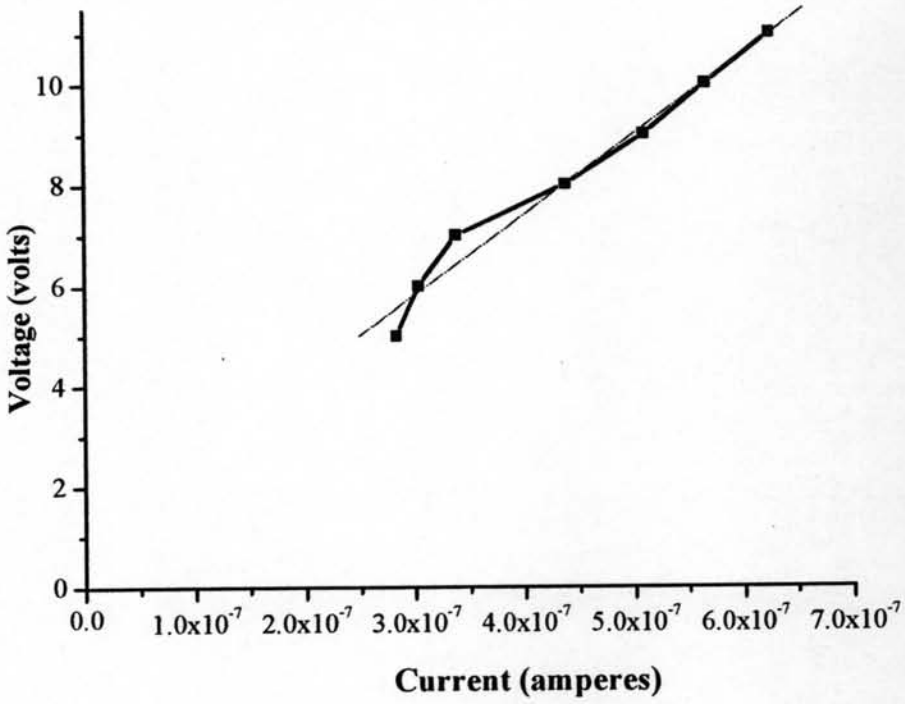

Figure J45 Surface resistance in linear range of C2,3-1.

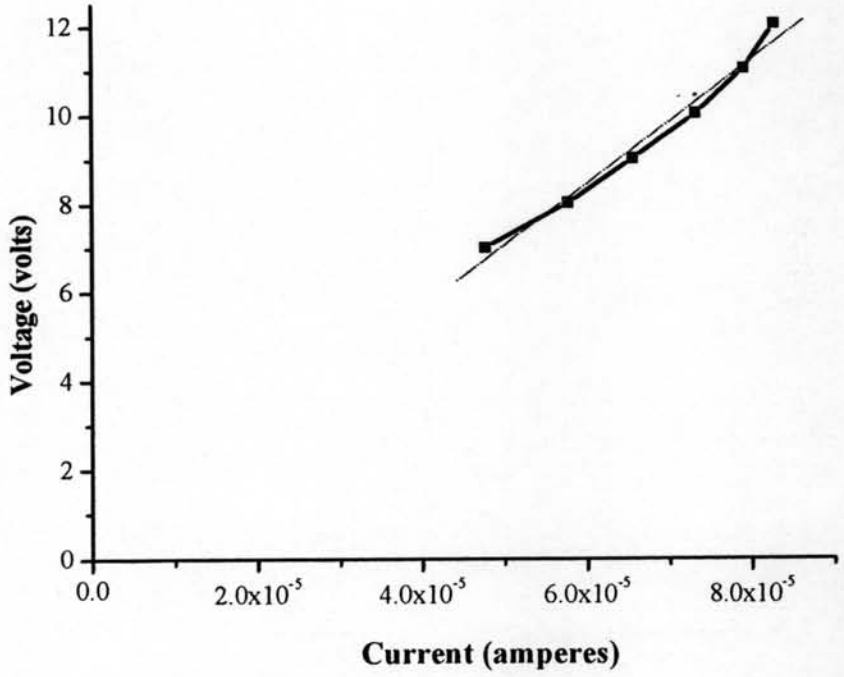

Figure J46 Surface resistance in linear range of C5,1-1.

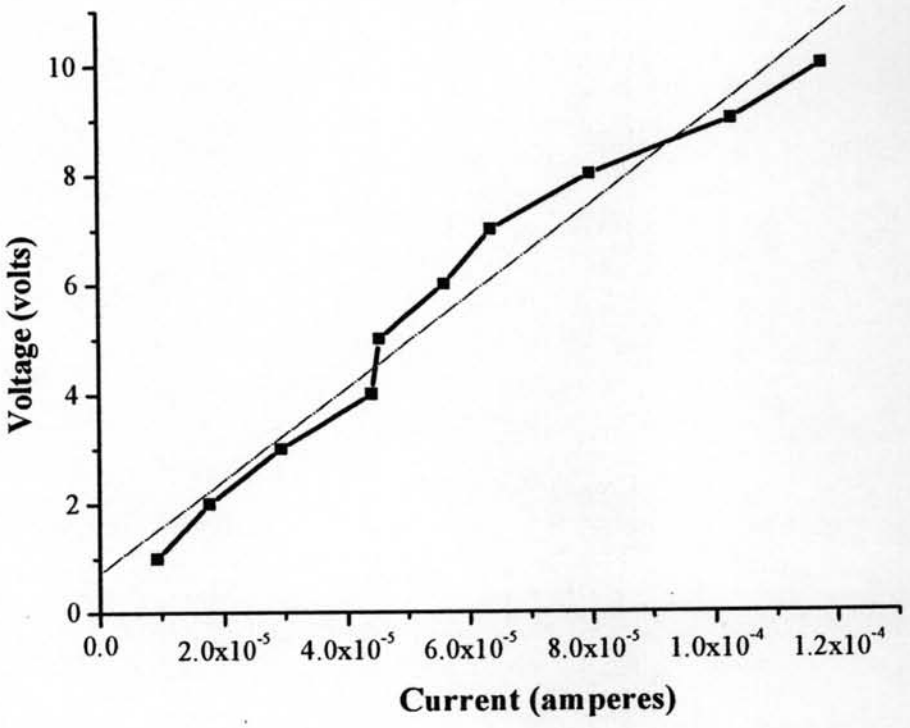

Figure J47 Surface resistance in linear range of C5,2-1.

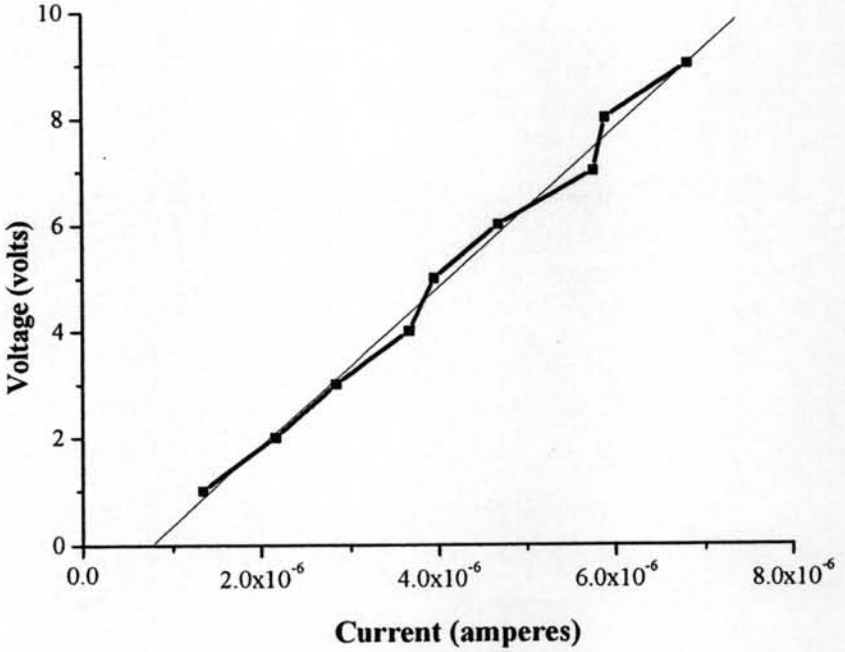

Figure J48 Surface resistance in linear range of C5,3-1.

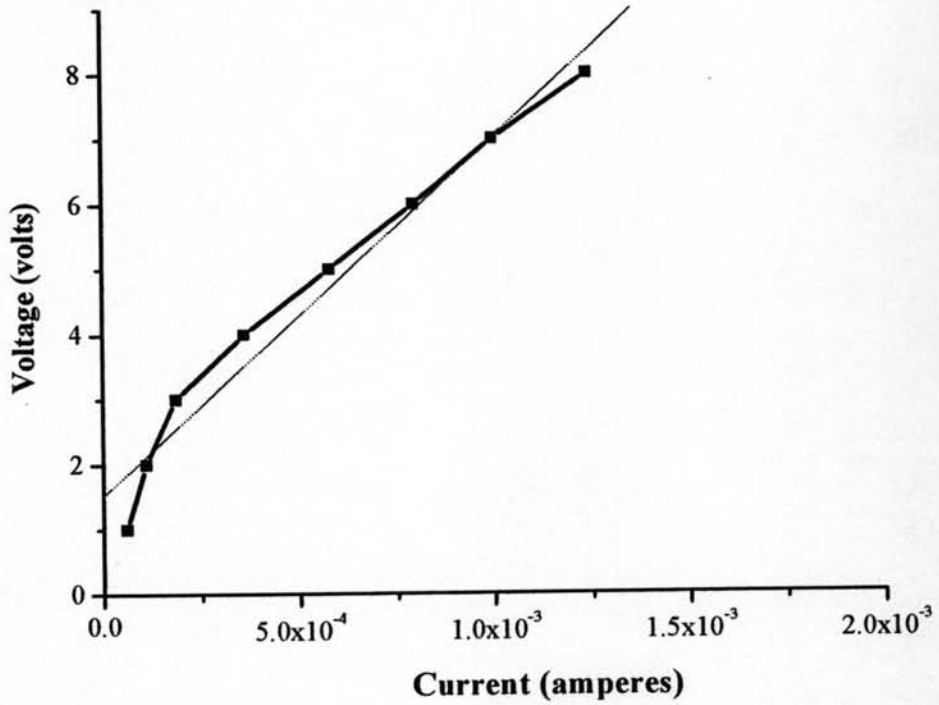

Figure J49 Surface resistance in linear range of C10,1-1.

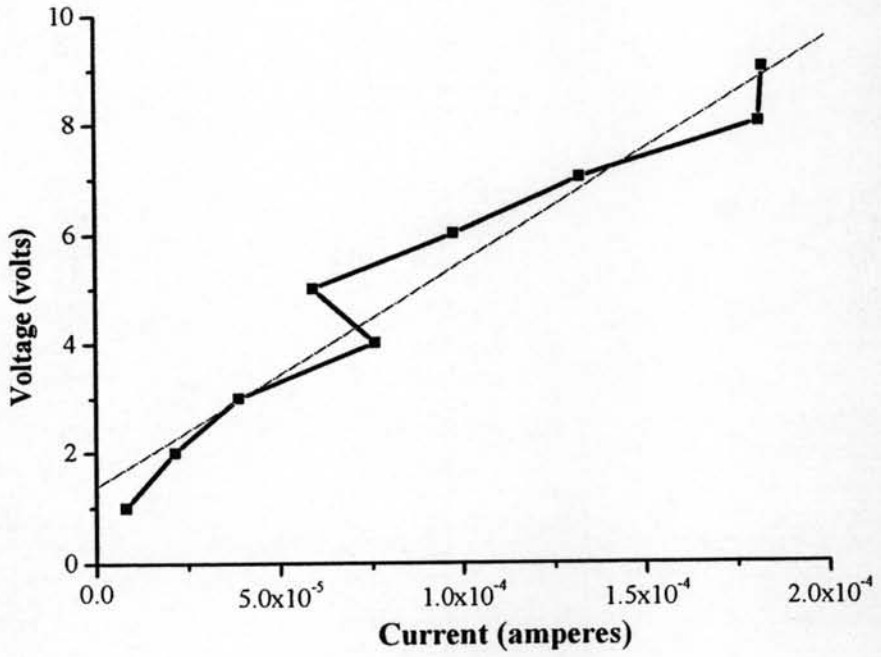

Figure J50 Surface resistance in linear range of C10,2-1.

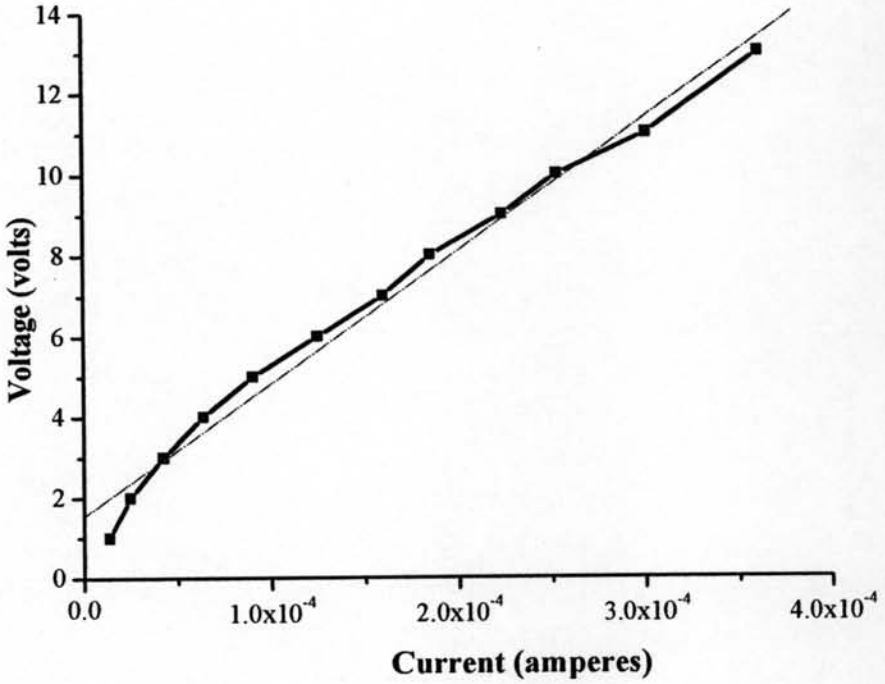

Figure J51 Surface resistance in linear range of C10,3-1.

CURRICULUM VITAE

Name: Ms. Sirinya Chantarak

Date of Birth: September 19, 1982

Nationality: Thai

University Education:

2001-2004 Bachelor Degree of Chemistry, Faculty of Science, Prince of Songkhla University, Songkla, Thailand

Publications:

1. Rukachaisirikul, V., Chantaruk, S., Tansakul, C.,Saithong, S., Chaicharernwimonkoon, L., Pakawatchai, C., Isaka, M., and Intereya, K. (2006). A Cyclopeptide from the Insect Pathogenic Fungus *Cordyceps* sp. BCC 1788. Journal Natural Products, *Note*, 69(2), 305-307.
2. Rukachaisirikul, V., Chantaruk, S., Pongcharoen, W., Isaka, M., and Lapanun, S. (2006) Chromone Derivatives from the Filaments Fungus *Lachnum* sp. BCC 2424. Journal Natural Products, *Note*, 69(6), 980-982.

Presentation:

1. Chantarak, S., and Magaraphan, R. (2007, February 11-15) Synthesis and Characterization of Polypyrrole Coated Latex Particles by Admicellar Polymerization. Poster presented at 29th Australasian Polymer Symposium, Tasmania, Australia.